Carbohydrate Polymer Technologies and Applications 9 (2025) 100644

Contents lists available at ScienceDirect

Carbohydrate Polymer Technologies and Applications

journal homepage: www.sciencedirect.com/journal/carbohydrate-polymer-technologies-and-applications

# Simultaneous screening and quantitation of human milk oligosaccharides by liquid chromatography—Mass spectrometry

Víctor Navarro-Esteve [a,b], Anna Zöchner [a,c], Marta Roca [d], Anna Parra-Llorca [e], Alba Moreno-Giménez [a], Laura Campos-Berga [a], María Jesús Vaya [f], Máximo Vento [a,e], Pilar Sáenz González [e], María Gormaz [e], Isabel Ten-Doménech [a,g,*], Julia Kuligowski [a,g,*], Guillermo Quintás [h,i]

[a] Neonatal Research Group, Health Research Institute La Fe, Avda Fernando Abril Martorell 106, 46026, Valencia, Spain
[b] Department of Analytical Chemistry, University of Valencia, Dr. Moliner 50, 46100 Burjassot, Spain
[c] Austrian Biotech University of Applied Sciences, Konrad Lorenz-Strasse 10, 3430 Tulln, Austria
[d] Analytical Unit, Health Research Institute La Fe, Avda Fernando Abril Martorell 106, 46026, Valencia, Spain
[e] Division of Neonatology, University & Polytechnic Hospital La Fe, Avda Fernando Abril Martorell 106, 46026, Valencia, Spain
[f] Blood Transfusion Center from the Valencian Community, Avda del Cid, 65-acc, 46014, Valencia, Spain
[g] Primary Care Interventions to Prevent Maternal and Child Chronic Diseases of Perinatal and Developmental Origin Network (RICORS-SAMID) (RD21/0012/0015), Instituto de Salud Carlos III, Madrid, Spain
[h] Centro de Investigación Biomédica en Red de Enfermedades Hepáticas y Digestivas (CIBERehd), Instituto de Salud Carlos III, Madrid, Spain
[i] Health and Biomedicine, Leitat Technological Center, Avda Fernando Abril Martorell 106, 46026, Valencia, Spain

ARTICLE INFO

*Keywords:*
Donor human milk (DHM)
Pasteurization
Newborn nutrition
Human milk oligosaccharide (HMO)

ABSTRACT

Human milk oligosaccharides (HMOs) are the third most abundant solid component in human milk (HM) and play a vital role in shaping the gut-microbiota and modulating neonatal immunity. Despite identifying 162 HMOs, clinical research primarily focused on a few. High throughput methods that encompass a broader range of HMOs for clinical studies remain limited. This study aimed to develop a novel method for simultaneously quantifying seven key HMOs (i.e., 2′-fucosyllactose, 3′-sialyllactose, 6′-sialyllactose, lacto-N-tetraose, lacto-N-fucopentaose I, lacto-N-difucohexaose I, disialyllacto-N-tetraose), and screening a broad HMO panel. The method utilizes hydrophilic interaction liquid chromatography coupled to mass spectrometry in polarity switching mode, and MS/MS annotation against the NIST Milk Oligosaccharide MS Library. Analysis of 40 HM samples pre- and post-pasteurization identified 110 HMOs. Additionally, the use of Feature-Based Molecular Networking for novel HMO structure identification is introduced. However, higher $MS^n$ fragmentation dimensions and complementary analytical techniques are necessary to enhance annotation confidence, structural assignments, and standardize HMO isolation. These findings highlight the diversity of HMOs and suggest implications for HM banks, where HMO profiles and maternal secretor phenotypes of donors are often unexamined.

*Abbreviations:* 2′-FL, 2′-fucosyllactose; 3-FL, 3-fucosyllactose; 3′-SL, 3′-sialyllactose; 6′-SL, 6′-sialyllactose; DHM, donor human milk; DSLNT, disialyllacto-N-tetraose; ESI, electrospray ionization; FBMN, Feature-Based Molecular Networking; FC, fold change; Fuc, fucose; FUT2, fucosyltransferase 2 gen; FUT3, fucosyltransferase 3 gen; Gal, galactose; Glc, glucose; GlcNAc, N-acetyl-glucosamine; GNPS, Global Natural Products Social Molecular Networking; HM, human milk; HMOs, human milk oligosaccharides; IS, internal standard; LC-MS, liquid chromatography-mass spectrometry; LNDFH I, lacto-N-difucohexaose I; LNFP I, lacto-N-fucopentaose I; LNT, lacto-N-tetraose; LSTc, sialyllacto-N-tetraose c; MFLNH III, monofucosyllacto-N-hexaose III; NEC, necrotizing enterocolitis; Neu5Ac, N-acetylneuraminic acid; Post, post-pasteurization; Pre, pre-pasteurization; QC, quality control; RSD, relative standard deviation; SPE, solid-phase extraction; SVRC, support vector regression correction; TFA, trifluoroacetic acid; UPLC, ultra-performance liquid chromatography.

* Corresponding authors at: Neonatal Research Group, Health Research Institute La Fe, Avda Fernando Abril Martorell 106, 46026, Valencia, Spain.

*E-mail addresses:* Victor.Navarro-Esteve@uv.es (V. Navarro-Esteve), anna.zoechner@gmail.com (A. Zöchner), marta_roca@iislafe.es (M. Roca), parra_ann@gva.es (A. Parra-Llorca), alba_moreno@iislafe.es (A. Moreno-Giménez), campos_lauber@gva.es (L. Campos-Berga), vaya_mar@gva.es (M.J. Vaya), maximo_vento@iislafe.es (M. Vento), saenz_pilgon@gva.es (P.S. González), gormaz_mar@gva.es (M. Gormaz), isabel.ten@uv.es (I. Ten-Doménech), julia.kuligowski@uv.es (J. Kuligowski), gquintas@leitat.org (G. Quintás).

https://doi.org/10.1016/j.carpta.2024.100644

Available online 20 December 2024
2666-8939/© 2024 The Author(s). Published by Elsevier Ltd. This is an open access article under the CC BY-NC license (http://creativecommons.org/licenses/by-nc/4.0/).

## 1. Introduction

Human milk (HM) is the gold standard for infant nutrition during the first semester, especially for preterm infants (Boquien, 2018). Breastfeeding has a positive effect on mothers' and infants' health (Louis-Jacques & Stuebe, 2020), but, in addition, specific milk constituents positively impact child neurodevelopment (Belfort & Inder, 2022). Therefore, HM characterization and quality control are critical in clinical nutrition (Catenza & Donkor, 2021).

However, HM composition is highly complex and dynamic. After lactose and lipids, the third most abundant solid component class naturally present in HM is HM oligosaccharides (HMOs), with concentrations ranging from 6 to 25 g $L^{-1}$ (Soyyılmaz et al., 2021). Notably, one of the key compositional distinctions between HM and cow's milk is the presence of HMOs, which are largely absent in the latter and in infant formula (Nijman et al., 2018).

HMOs are synthesized by glucosyltransferases in the mammary gland and they are composed of five monosaccharide units: glucose (Glc), galactose (Gal), fucose (Fuc), N-acetylglucosamine (GlcNAc), and N-acetylneuraminic acid (Neu5Ac), with the latter being the main form of sialic acid in humans (Q. Chen et al., 2024). Up to 162 structurally different HMOs have been identified and characterized in HM so far (Urashima et al., 2018), although 85 additional, not fully characterized HMOs have been described (Noll et al., 2016). While content and variability of HMOs change across lactation (Soyyılmaz et al., 2021), the most important source of variance in HMO production between individuals is ascribed to genetic variations on the fucosyltransferase 2 (FUT2) and 3 (FUT3) genes, known as secretor and Lewis genes, respectively. Mothers who carry inactivating mutations in FUT2 or FUT3 are referred to as non-secretors or Lewis negative, respectively, representing ~20 % and ~9 % of the European population (Samuel et al., 2019).

Beneficial effects of HMOs such as their prebiotic and immunomodulator effects have been described (Okburan & Kızıler, 2023). Moreover, there is increasing evidence that HMO consumption has an impact on child development including growth (Larsson et al., 2019) and food responsiveness (Plows et al., 2020). Furthermore, HMOs play a vital role in the development of the infant's gut microbiome, and immune function (Plaza-Díaz et al., 2018), in the regulation of the microbiome and the prevention of gastrointestinal disorders (Marcobal et al., 2010; Nolan et al., 2020). Low concentrations of some HMOs have been associated with a higher risk of developing necrotizing enterocolitis (NEC) (Autran et al., 2018), a serious gastrointestinal condition in the premature neonate with high mortality and long-term impairments (Duchon et al., 2021).

In cases where there is an insufficient supply of HM, the preferred option for feeding preterm infants is donor human milk (DHM) rather than preterm formula (Underwood, 2013). However, prior to its administration and to minimize the potential risk of transmitting infectious agents and warrant its safety, DHM is manipulated following stringent protocols in HM banks that involve pasteurization, freezing, and storage. These procedures compromise the integrity and degrade bioactive components such as enzymes and immune cells. Previous results restricted to a subset of 33 HMOs indicated that pasteurization does not affect HMO concentrations (Hahn et al., 2019). However, further research is necessary to expand the range of HMOs studied in stability studies. In light of this, there is a pressing need for analytical methods enabling a thorough characterization of the HMO profile.

Several instrumental strategies for the qualitative and quantitative determination of HMOs have been developed (Auer et al., 2021), being the most frequently used technique ultraperformance liquid chromatography (UPLC) coupled to mass spectrometry (MS) or fluorescence detection (Auer et al., 2021). However, due to their complex structure and chemical diversity, and the limited availability of HMO standards, clinical studies have typically focused on quantitation of subsets of HMOs covering typically 2–23 analytes (Csernák et al., 2020; J. Li et al., 2022; Nijman et al., 2018; Plows et al., 2021; Sprenger et al., 2017; Tonon, Miranda et al., 2019; M. Wang et al., 2020).

In untargeted UPLC-MS analysis, the term 'annotation' refers to the putative identification of a metabolite for which the assignment of its structure is highly likely. Based on physicochemical properties, spectral similarity, and availability of chemical reference standards, different levels of annotation can be established (Sumner et al., 2007). Due to the limited availability of chemical reference standards required to reach the highest level of annotation, biological databanks and spectral databases play a pivotal role in metabolite annotation. Hence, experimentally acquired MS and $MS^n$ data of a given metabolite are matched against databases such as the HMDB (https://hmdb.ca/), METLIN (https://metlin.scripps.edu), or the NIST Milk Oligosaccharide MS Library (Remoroza et al., 2018, 2020). On the other hand, molecular networking has recently become a key method to annotate, visualize, and connect molecules using their MS/MS spectra according to their similarities, either against compound spectra gathered in MS/MS libraries (annotation) or between them (connection), through the assumption that structurally related molecules display similar MS/MS spectra (Nothias et al., 2020). The structural elucidation of most HMOs using MS/MS is challenging due to the simultaneous occurrence of two distinct types of fragmentations: glycosidic and cross-ring cleavages. In this regard, Remoroza et al. (2018, 2020) have developed a mass spectral library for HMOs, which comprises consensus spectra of compounds annotated through multiple data analysis techniques. In this context, the recent work of Remoroza et al. (2018, 2020) presents an opportunity to enhance analytical methods for HMO characterization.

Our hypothesis suggests that the comprehensive profile of HMOs can be effectively captured in a single hybrid UPLC-MS/MS analysis. In addition, leveraging recently developed networking platforms allows an in-depth exploration and further understanding of the interactions and structures of HMOs.

## 2. Materials and methods

### 2.1. Human milk samples

DHM samples were provided by 11 healthy volunteers admitted after routine screening to the HM bank (Banco de Leche Materna de la Comunidad Valenciana, Valencia, Spain). Demographics of donors and their infants are shown in **Table S1**. DHM was collected using breast pumps according to the hospital staff's instructions. Milk was stored at −20 °C and transported to the HM bank within three weeks after extraction. At the HM bank, bottles from the same donor were pooled (typically when 1.5–2 L of milk was reached), constituting a batch from this donor. Between one and nine batches of HM from different donors at different time points after delivery were provided. In total, 40 DHM batches were prepared, of which aliquots directly before and after Holder pasteurization (i.e., heat treatment at 62.5 °C during 30 min followed by rapid cooling to 4 °C) were collected and stored at −80 °C. For each batch, the mean elapsed time between the first and last expression of HM was calculated, and this time point was adopted as an approximation to the sample collection time with respect to delivery (see **Table S1**). 82.5 % of the pools comprised bottles collected within a maximum of three weeks.

The study was approved by the Ethics Committee for Biomedical Research of the Health Research Institute La Fe, University and Polytechnic Hospital La Fe (Valencia, Spain) with registry # 2019-289-1, and all methods were performed in accordance with relevant guidelines and regulations. Written informed consents were obtained from lactating mothers prior to collection of samples, and demographic and clinical information.

### 2.2. Standards and reagents

LC–MS grade acetonitrile (>99.9 %) was obtained from Scharlau

(Barcelona, Spain), formic acid (≥95 %), trifluoroacetic acid (TFA) (≥99 %), ammonium acetate (≥98 %), and chloroform (≥ 99.5 %) from Sigma-Aldrich Química SL (Madrid, Spain). Ethanol (≥ 99.5 %) and LC-MS grade methanol (>99.9 %) were purchased from Labkem (Barcelona, Spain). Ultra-pure water was generated employing a Milli-Q Integral Water Purification System from Merck Millipore (Darmstadt, Germany). 3′-Sialyllactose (3′-SL) sodium salt (≥98 %), lacto-N-tetraose (LNT) (≥95 %), lacto-N-fucopentaose I (LNFP I) (≥95 %), 2′-fucosyllactose (2′-FL) (≥95 %), 3-fucosyllactose (3-FL) (95 %), lacto-N-difucohexaose I (LNDFH I) (≥95 %), and monofucosyllacto-N-hexaose III (MFLNH III) (90 %) were acquired from Carbosynth (Bratislava, Slovakia). 6′-Sialyllactose (6′-SL) sodium salt (≥97 %), disialyllacto-N-tetraose (DSLNT) (≥95 %), and isomaltotriose DP3 were obtained from Merck (Darmstadt, Germany). This panel covered the most abundant neutral (i.e., 2′-FL, 3-FL, LNT, LNFP I, LNDFH I) and acidic HMOs (3′-SL and 6′-SL), as well as DSLNT, since this latter HMO has been established to be associated with NEC development in premature infants (Masi et al., 2021).

### 2.3. Preparation of stock and standard solutions

Individual stock solutions of standards (i.e.,12.5 mmol $L^{-1}$ 2′-FL, 4.4 mmol $L^{-1}$ LNT, 5.3 mmol $L^{-1}$ LNFP I, 1 mmol $L^{-1}$ LNDFH I, 7.2 mmol $L^{-1}$ 3-FL, 1 mmol $L^{-1}$ 3′-SL, 1.6 mmol $L^{-1}$ 6′-SL, and 1 mmol $L^{-1}$ DSLNT) were prepared in water and stored at −20 °C. By mixing appropriate volumes of these individual solutions, a working solution with 600 μmol $L^{-1}$ of 2′-FL and LNT; 300 μmol $L^{-1}$ of LNFP I and LNDFH I; and 80 μmol $L^{-1}$ of 3-FL, 3′-SL, 6′-SL, and DSLNT in $H_2O$ was prepared. A calibration curve was then prepared by serial dilution in water:acetonitrile (1:1, v/v) with concentrations ranging from 3 to 600 μmol $L^{-1}$ depending on the HMO, and with isomaltotriose as internal standard (IS) (Csernák et al., 2020) at a concentration of 8 μmol $L^{-1}$.

### 2.4. Extraction and purification of HMOs

HMO extraction was carried out following a previously described protocol (Remoroza et al., 2018) with some modifications. Briefly, HM samples were thawed at room temperature and mixed by inverting ten times. An aliquot of 50 μL of HM was withdrawn, diluted with 200 μL of Milli-Q $H_2O$ and centrifuged at 14.000 x g at 4 °C for 30 min. 200 μL of the liquid layer were mixed with 800 μL of chloroform:methanol (2:1 v/v) and centrifuged at 14.000 x g at 4 °C for 30 min. Then, 300 μL of the aqueous phase were transferred and mixed with 600 μL of ethanol. The resulting mixture was kept at 4 °C overnight for protein precipitation and then centrifuged at 14.000 x g at 4 °C for 30 min. The liquid phase was carefully collected and evaporated to dryness with a miVac centrifugal vacuum concentrator (Genevac LTD, Ipswich, UK) at 50 °C. The dry residue was redissolved in 192 μL of $H_2O$ and 8 μL of a 250 μmol $L^{-1}$ IS solution prior to solid phase extraction (SPE). A Thermo Scientific™ (Rockwood TN, USA) HyperSep Hypercarb SPE 96-Well Plate (50 mg bed weight) was pre-conditioned with 500 μL water, 500 μL 80 % v/v acetonitrile with 0.1 % v/v TFA, and 500 μL water. After sample loading, unwanted, weakly bound components were washed with 600 μL of water. Then, neutral and acidic HMOs were jointly eluted with 400 μL of 20 % v/v acetonitrile (0.05 % v/v TFA) and 400 μL of 40 % v/v acetonitrile (0.05 % v/v TFA). The eluted samples were evaporated to dryness in a miVac centrifugal vacuum concentrator and reconstituted in 250 μL of 50 % v/v acetonitrile. In addition, a blank extract was prepared following the steps described for HM samples but replacing HM with water. A pooled quality control (QC) sample was prepared by mixing 130 μL of each HM sample extract. Accuracy and precision levels of the method, the SPE extraction yield, and matrix effect were evaluated in triplicate by spiking a HM sample, a pre-processed HM sample prior to SPE, and a recovered HM extract after SPE, respectively.

### 2.5. HILIC-MS/MS method

For HMO screening, a UPLC system coupled to an Orbitrap QExactive Plus MS (ThermoFisher, Waltham, MA, USA) was employed. Chromatographic conditions were adapted from elsewhere (Remoroza et al., 2018). An ACQUITY Glycoprotein BEH Amide pre-column (1.7 μm, 2.1 × 5 mm, 130 Å, Waters, Milford, MA, USA) connected to an ACQUITY Glycoprotein BEH Amide column (1.7 μm, 2.1 × 100 mm, 130 Å, Waters) was installed on a Vanquish UHPLC Binary Pump (Thermo Fisher). The flow rate was set to 600 μL $min^{-1}$ and the column temperature to 35 °C. The injection volume was 5 μL. The composition of the two mobile phases was: 10 mmol $L^{-1}$ ammonium formate in $H_2O$ with 0.1 % v/v formic acid (A) and 99.9 % v/v acetonitrile with 0.1 % v/v formic acid (B). The gradient elution program was performed as follows: during 0.75 min 95 % v/v B; from 0.75 to 5 min linear gradient from 95 % v/v to 80 % v/v B; from 5 to 30 min linear gradient from 80 % v/v to 50 % v/v B followed by 2.5 min of column washing with a linear gradient from 50 % v/v to 2 % v/v B including column re-equilibration with 95 % v/v B. During the column washing, the flow rate was set at 250 μL $min^{-1}$. The total runtime was 32.5 min. MS detection was carried out in electrospray ionization (ESI) alternating positive and negative modes (polarity switching) with the ion source voltage set to ±3.5 kV; the capillary temperature to 250 °C; the sheath gas to 15 (arbitrary units); and the auxiliary gas to 10 (arbitrary units). Two inclusion lists (one per polarity) were constructed including the precursor mass-to-charge ratios ($m/z$) of all HMO adducts reported for HM that are listed in the NIST Milk Oligosaccharide MS Library (Remoroza et al., 2020). An exclusion list was also constructed including $m/z$ peaks detected in a blank injection. MS/MS spectra were acquired using the beam-type collision cell fragmentation higher energy dissociation (HCD), being the normalized collision energy (NCE) 25 %.

80 DHM sample extracts (40 pre- and 40 post-pasteurization) were injected in random order within four different batches (i.e., four measurement days). QC samples were injected after every six samples and twice at the beginning and end of each batch for assessment and correction of instrumental performance (Broadhurst et al., 2018). The blank extract was injected once at the end of the measurement sequence to identify signals from other than biological origin (Martínez-Sena et al., 2019).

### 2.6. LC-MS data processing

2′-FL, 3-FL, 3′-SL, 6′-SL, LNT, LNFP I, LNDFH I, and DSLNT were quantified using the Xcalibur Quan Browser Software version 4.1 (ThermoFisher) using linear regression curves and relative responses (i.e., peak areas of compounds normalized to peak area of the IS). For HMO screening, chromatograms acquired using $ESI^+$ and $ESI^-$ modes were processed separately but following the same workflow. Centroid UPLC-MS raw data were converted to mzXML and ms2 formats employing ProteoWizard (http://proteowizard.sourceforge.net) (Kessner et al., 2008). Peak detection, integration, deconvolution, alignment, and pseudospectra identification were carried out using XCMS running in R 4.0.3 (Tautenhahn et al., 2012). The feature detection method was centWave; the maximal tolerated $m/z$ deviation in consecutive scans was 5 ppm; the minimum and maximum peak width were 10 s and 30 s, respectively; the signal/noise threshold was set to 4; the mzdiff (minimum difference in $m/z$ for peaks with overlapping retention times) was −0.01; the peak limits used for integration were found through descent on the Mexican hat filter data; the prefilter peaks and intensity were set to 3 and 1000, respectively, and the noise filter to 100. The retention time correction method was obiwarp, being the step size used for profile generation 1 Da Alignment was performed with the density method applying the following parameters: mzwid (width of overlapping $m/z$ slices to use for creating peak density chromatograms and grouping peaks across samples) of 0.025; bandwidth (standard deviation or half width at half maximum) was set to 5; minimal fraction of samples was

set to 0.1. Peak filling was performed using the *chrom* method. Annotation of isotopes and adducts and their grouping was performed following the CAMERA workflow.

The resulting peak tables were used for HMO annotation and data analysis in MATLAB 2021a (Mathworks Inc., Natick, MA, USA). MS/MS spectra and retention times (RTs) from HM sources and their respective information were imported from the NIST Milk Oligosaccharide MS Libraries accessed via the links available at (Remoroza et al., 2018) (https://chemdata.nist.gov/dokuwiki/doku.php?id=peptidew:lib:oligosaccarides) and (Remoroza et al., 2020) (https://chemdata.nist.gov/dokuwiki/doku.php?id=%20peptidew:lib:nonhumanmilk). A list of HMOs considered for annotation is presented in **Table S2**. RTs of available HMO standards in this study (i.e., 2′-FL, 3-FL, 3′-SL, 6′-SL, LNT, LNFP I, LNDFH I, and DSLNT) under the selected chromatographic conditions ($RT_{exp}$) and those of the NIST library ($RT_{NIST}$) were used to build a linear model (i.e., $RT_{exp} = 1.86 + 0.54 \cdot RT_{NIST}$, $R^2$=0.992). The model was used to estimate the RTs of putatively annotated HMOs based on MS/MS data ($RT_{pred}$) and their reference $RT_{NIST}$. Spectral matching and annotation were performed using in-house written MATLAB scripts as described elsewhere (Ten-Doménech et al., 2020) with the following parameters: *m/z* accuracy error between experimental and database parent ion, 10 ppm; absolute difference between $RT_{exp}$ and $RT_{pred}$ <0.3 min; difference in RT between parent ion and MS/MS spectra, 0.5 min; intensity threshold to remove low intensity MS/MS signals, absolute intensity <0.1 AU or relative intensity <0.001 % of base peak; MS/MS spectra normalization, base peak; minimum number of ions in each experimental and database spectrum, 3; minimum number of matching ions between experimental and database spectrum, 2; maximum number of potential matches to retrieve, 5; $^{13}C$ de-isotoping was not performed. All automatic annotations were manually reviewed and validated by visual inspection of MS/MS spectra. Within-batch effect elimination was performed using Quality Control – Support Vector Regression Correction (QC-SVRC) (Kuligowski et al., 2015) after selection of SVR hyperparameters (Sánchez-Illana, Pérez-Guaita et al., 2018). Between-batch effect correction was performed by normalizing to the median of each QC feature across all batches (Sánchez-Illana, Piñeiro-Ramos et al., 2018). Features for which the relative standard deviation (%RSD) of QCs was greater than 25 in more than one batch after QC-SVRC and features for which the median values in QCs were lower than 6 times the median value in blanks were excluded from further data analysis.

### 2.7. Molecular networking and spectral library search

A molecular network was created with the Feature-Based Molecular Networking (FBMN) workflow (Nothias et al., 2020) on Global Natural Products Social Molecular Networking (GNPS) (http://gnps.ucsd.edu, (M. Wang et al., 2016)). The MS data was filtered by removing all MS/MS fragment ions within +/- 17 Da of the precursor *m/z*. MS/MS spectra were window filtered by choosing only the top 6 fragment ions in the +/- 50 Da window throughout the spectrum. The precursor ion mass and the MS/MS fragment ion tolerances were set to 0.02 Da. A molecular network was then created where edges were filtered to have a cosine score above 0.7 and more than 5 matched peaks. Further, edges between two nodes were kept in the network if and only if each of the nodes appeared in each other's respective top five most similar nodes. Finally, the maximum size of a molecular family was set to 100, and the lowest scoring edges were removed from molecular families until the molecular family size was below this threshold. The spectra in the network were then searched against the NIST Milk Oligosaccharide MS Library. The library spectra were filtered in the same manner as the input data. All matches kept between network spectra and library spectra were required to have a score above 0.6 and at least 2 matched peaks. The molecular networks were visualized using Cytoscape software (Shannon et al., 2003).

### 2.8. Statistical analysis and data availability

Visualization and statistical analysis was performed using built-in functions in MATLAB and the PLS Toolbox 9.3 (Eigenvector Research Inc., Wenatchee, USA). For the pasteurization study, the Kolmogorov normality test and the Wilcoxon signed-rank test were applied. Strength of monotonic relationship between pairs of variables (e.g., HMO content and postnatal age) was assessed through the Pearson linear correlation coefficient. Diversity of HMOs within a sample was assessed using the Simpson's Index of Diversity (1-*D*), where *D* was defined as:

$$D = \frac{\sum n(n-1)}{N(N-1)} \quad (1)$$

being *n* the concentration of a particular HMO in the sample; and N the total concentration of HMOs. Thus, the higher the value for this index (1-*D*), the higher the HMO diversity.

The MS data has been deposited on MassIVE public repository with code: MSV000090546 (Username: MSV000090546_reviewer; Password: HMOs_reviewers). The molecular networking job can be publicly accessed at https://gnps.ucsd.edu/ProteoSAFe/status.jsp?task=ea1bb50d941a43e796c27ffd8a733a6c.

### 2.9. Literature search

The PubMed database was searched using the query "Human Milk Oligosaccharides liquid chromatography mass spectrometry" published between January 1, 2018, to November 1, 2024, retrieving a total of 77 results. After an initial review of the abstracts and a visual inspection of the 'Materials and methods' sections, 46 out of 77 articles were excluded based on the following criteria: (i) Not an original article (review article) (*N*= 2); (ii) Not available in English (*N*= 1); (iii) Not related to HMO analysis (*N*= 14); (iv) Not from human origin but from other mammals or plants (e.g., mouse milk, camel milk, bovine milk, soy, etc.) (*N*= 10); (v) Did not use LC-MS for HMO analysis (*N*= 7); (vi) Analyzed HMOs in matrices other than HM (e.g., amniotic fluid, maternal circulation) (*N*= 4); (vii) Focused on O/N-glycans rather than HMOs (*N*= 5); (viii) Focused exclusively on HMOs with high degree of polymerization (*N*= 1); (ix) Focused on free and bound sialic acids (*N*= 1); (x) Focused on structural characterization of HMOs without application to HM samples (*N*= 1). The remaining 31 articles were kept for comparison and information regarding sample preparation and analysis as well as the study cohort was extracted.

## 3. Results and discussion

### 3.1. Tailored UPLC-MS method development for HMO analysis

A novel method for the detection of a broad panel of HMOs and the quantification of a subset of selected HMOs for use in clinical studies was developed (see Fig. 1). The method involved a sample preparation step using SPE to achieve a quantitative extraction of HMOs, allowing for efficient processing of up to 96 sample in parallel using a 96-well plate format. Sample analysis was performed using polarity switching to reduce the sample analysis time (32.5 min), aided by an inclusion list constructed from the information contained in the NIST Milk Oligosaccharide MS Library to improve the MS/MS fragmentation coverage of relevant ions. Additionally, three complementary data processing strategies were employed for a more in-depth exploration of HMOs profiles: (1) HMO quantitation, (2) screening, and (3) molecular networking.

#### 3.1.1. HMO quantitation

**Figure S1** shows total ion and extracted ion chromatograms of HMOs selected for quantitation of a standard mixture and a QC sample in $ESI^+$ mode. 3-FL and LNDFH I showed two peaks caused by the presence of anomers that were separated by HILIC. For 3-FL, both peaks were jointly

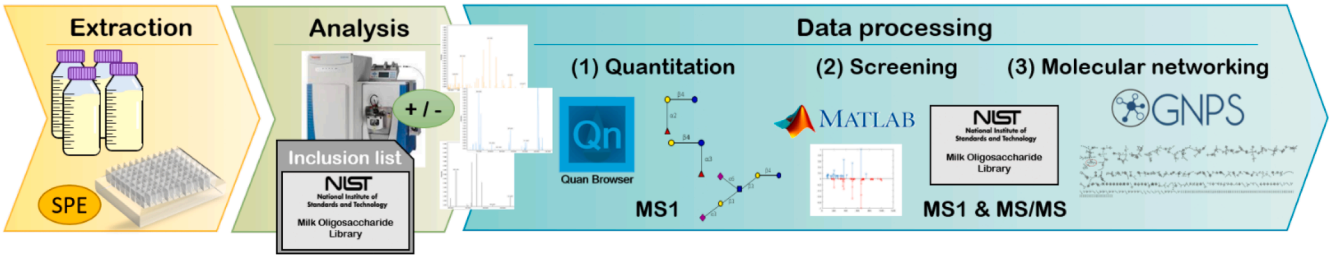


**Fig. 1.** Flow chart of the developed methodology for HMO analysis.

considered for calibration, whereas for LNDFH I only the most intense one was used. For the quantitation of 2′-FL, 3-FL, 3′-SL, 6′-SL, LNT, LNFP I, LNDFH I, and DSLNT, linear regression curves with relative response covering two to three orders of magnitude were calculated showing $R^2 \geq 0.992$ for all HMOs (see Table 1). Nonetheless, quantification of 3-FL in HM samples was not feasible due to its elution during the SPE washing step, in agreement with previous studies (Gu et al., 2021). Table 1 shows method recovery, extraction yield, matrix effect, and median concentrations of the selected HMOs in DHM samples before and after pasteurization. Overall, acceptable method recoveries (between 70 and 116 %) and extraction yields were obtained, although the SPE step seemed to compromise the yield of certain acidic HMOs. No relevant matrix effect was observed with recoveries ranging from 93 to 131 %. Neutral HMOs (i.e., 2′-FL, LNT, LNFP I, and LNDFH I) were found at higher concentrations than acidic HMOs (i.e., 3′-SL, 6′-SL, and DSLNT), being 2′-FL the most abundant, followed by LNT, LNDFH I, and LNFP I. Regarding acidic HMOs, 6′-SL was more abundant in DHM samples than 3′-SL and DSLNT. These results are in agreement with previous studies, which included a notably larger number of participants (J. Li et al., 2022; Siziba et al., 2021), although other studies reported LNT to be the most abundant HMO (Fan et al., 2023).

**Figure S2** depicts the correlations between pairs of HMOs in DHM samples. Results showed statistically significant ($p$-value $< 0.001$) positive correlations between several HMOs. 2′-FL was positively correlated with other FUT2 dependent HMOs (i.e., LNFP I), but not with core structures such as LNT and acidic HMOs. This observation agrees with the findings of Sprenger et al. (Sprenger et al., 2017), that indicated that the synthesis of 2′-FL and LNT is not co-regulated.

### 3.1.2. HMO screening

In addition to the quantitation of seven HMOs, this method allows HMO screening. HMO annotation is especially challenging considering the high number of structurally similar HMOs covering a wide range of concentrations in HM samples. Moreover, most HMOs have structural isomers with the same molecular formula, differing in branching points and/or distribution of the different monosaccharide units.

The accuracy of peak detection, integration, and alignment during the peak table generation was assessed by comparing peak area values estimated using the XCMS-approach with those obtained by manual chromatographic peak integration (Xcalibur) for a subset of HMOs (see **Figure S3**). Excellent agreement between both methods with correlation coefficients >0.98 was achieved.

A total of 42,552 and 38,220 LC-MS features were initially detected in $ESI^+$ and $ESI^-$ ionization modes and they were reduced to 7363 and 11,705 after clean-up (i.e., removal of features with RSD > 25 % in QCs and features with median values in QCs lower than 6 times the median value in blanks), from which 726 and 372 were initially annotated as HMOs or their fragments and adducts, respectively. Fig. 2 shows the distribution of annotated HMOs in the $m/z$-retention time space. The correlation between the experimental and reference MS/MS spectra in terms of $m/z$ values and intensities was assessed through the calculation of the mean dot product (Hutchins et al., 2018). Annotated entries were carefully revised in terms of spectral match, diagnostic $m/z$ ions, and RT. As a result, 103 and 49 unique HMOs in positive and negative ionization mode, respectively, overall comprising 110 unique HMOs, could be annotated (**Table S3**). HMOs with high oligomeric structures showed a high spectral match due to a rich fragmentation pattern (e.g., **Table S3**, entry #108). Moreover, this method enabled putative annotation with a reliable spectral match even with limited spectral information for some metabolites (e.g., **Table S3**, entry #103). However, it should be noted that, the combined use of a UPLC-MS/MS method and a library dependent spectral matching algorithm have certain methodological limitations and hence, including additional dimensions, e.g., higher $MS^n$ fragmentation dimensions, ion mobility data (Peterson & Nagy, 2021), and/or complementary analytical techniques (Abikhodr et al., 2024) or sample processing (Porfirio et al., 2020) would further increase confidence in the annotation and support structural assignments.

### 3.1.3. HMO molecular networking

In addition to annotation based on matching with the NIST Milk Oligosaccharide MS Library, the FBMN workflow of the GNPS platform was employed to potentially enlarge the number of annotated HMOs. Fig. 3 (top) shows the FBMN of HMOs in the positive mode. 256 nodes were annotated, which resulted in 70 unique HMOs summarized in **Table S4**. Among them, 53 HMOs were successfully annotated by both strategies (i.e., spectral matching and FBMN workflow), and 17 HMOs were exclusively annotated by the FBMN workflow.

By comparing the corresponding structures and adducts of annotated HMOs and with help of the NIST Milk Oligosaccharide MS Library, connections between nodes were inspected to establish changes in terms of adduct/exchange/removal of monosaccharide units between the corresponding HMOs (see Fig. 3, bottom). **Figure S5** shows the frequency of $m/z$ differences of edges in the FBMN and for networks containing nodes annotated as HMOs. The corresponding changes ascribed to these latter networks are presented in **Table S5**. Note that not all connections could be explained since the number of annotated nodes involved was insufficient. After compiling the potential changes associated with certain connections, its potential use to elucidate unknown nodes in the network was evaluated. As shown in Fig. 3 (bottom), two unknown nodes (in red) could be potentially ascribed to the ammonium adduct of sialyllacto-N-tetraose c (LSTc). This approach could be used to expand the library entries (as for the ammonium adduct of LSTc) and, more interestingly, to unveil potential HMO structures not included in the library or not previously reported. This approach is thought to serve as a supportive tool for generating hypothesis and requires subsequent validation through follow-up experiments to enhance confidence in the findings.

### 3.1.4. Methodological comparison with published literature

Table 2 presents a summary of thirty-one LC-MS methodologies adopted for HMO analysis published between January 1, 2018, and November 1, 2024. As it can be seen, sample preparation methods for HMO analysis vary widely. The use of cold centrifugation for fat removal and an organic solvent (e.g., ethanol) for protein removal are common practice. Reduction of HMOs and SPE purification are also relatively common, as they help mitigate subsequent challenges in the

**Table 1**
Parameters used for the quantification of eight HMOs and observed concentrations in DHM samples before (Pre) ($N$= 40) and after pasteurization (Post) ($N$= 40).

| HMO | Structure | Mol. Formula | Adduct | RT Mean ± SD (min) | Calibration range (μmol $L^{-1}$) | $R^2$ | Method recovery (%) | Extraction yield, Recovery (%) | Matrix effect, Recovery (%) | DHM-Pre Median (IQR) (μmol $L^{-1}$) | DHM-Post Median (IQR) (μmol $L^{-1}$) |
|---|---|---|---|---|---|---|---|---|---|---|---|
| 2′-FL | 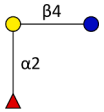 | $C_{18}H_{32}O_{15}$ | $[M+NH_4]^+$ | 8.51 ± 0.05 | 19 – 600 | 0.998 | 116 ± 19 | 96 ± 6 | 131 ± 2 | 4675 (1478) | 4825 (2029) |
| 3-FL | 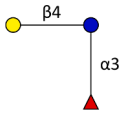 | $C_{18}H_{32}O_{15}$ | $[M+NH_4]^+$ | 9.16 ± 0.03 | 3 – 80 | 0.997 | 0 | 0 | 118 ± 4 | NA | NA |
| 3′-SL |  | $C_{23}H_{39}NO_{19}$ | $[M+H]^+$ | 10.67 ± 0.08 | 3 – 80 | 0.9990 | 70 ± 5 | 66 ± 6 | 106.9 ± 0.6 | 163 (87) | 169 (70) |
| 6′-SL |  | $C_{23}H_{39}NO_{19}$ | $[M+H]^+$ | 11.54 ± 0.08 | 3 – 80 | 0.9990 | 94 ± 7 | 87 ± 2 | 103 ± 2 | 253 (362) | 287 (395 |
| LNT | 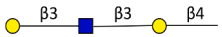 | $C_{26}H_{45}NO_{21}$ | $[M+H]^+$ | 11.77 ± 0.05 | 19 – 600 | 0.992 | 86 ± 11 | 95 ± 8 | 93 ± 5 | 2869 (1948) | 2873 (2063) |
| LNFP I | 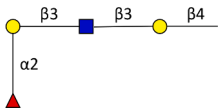 | $C_{32}H_{55}NO_{25}$ | $[M+H]^+$ | 13.47 ± 0.05 | 9 – 300 | 0.9990 | 107 ± 6 | 95 ± 3 | 112 ± 2 | 839 (1066) | 817 (976) |
| LNDFH I | 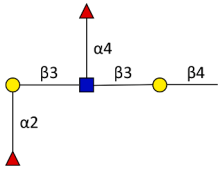 | $C_{38}H_{65}NO_{29}$ | $[M+H]^+$ | 15.90 ± 0.05 | 9 – 300 | 0.9990 | 103 ± 5 | 94 ± 8 | 113 ± 3 | 1642 (1128) | 1615 (1009) |
| DSLNT | 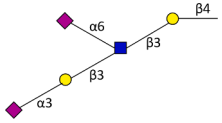 | $C_{48}H_{79}N_3O_{37}$ | $[M+H]^+$ | 17.67 ± 0.09 | 3 – 80 | 0.998 | 75 ± 1 | 67 ± 9 | 104 ± 7 | 81 (71) | 74 (71) |
| Isomaltotriose, DP3 | 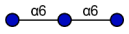 | $C_{18}H_{32}O_{16}$ | $[M+NH_4]^+$ | 10.81± 0.09 | – | – | | | | – | |

Note: 2′-fucosyllactose (2′-FL); 3-fucosyllactose (3-FL); 3′-sialyllactose (3′-SL); 6′-sialyllactose (6′-SL); lacto-N-tetraose (LNT); lacto-N-fucopentaose I (LNFP I); lacto-N-difucohexaose I (LNDFH I); disialyllacto-N-tetraose (DSLNT); retention time (RT), standard deviation (SD); interquartile range (IQR); symbol nomenclature based on the recommendations by the consortium for functional glycomics (i.e., ▲ = Fucose (Fuc), ● = Galactose (Gal), ● = Glucose (Glc), ◆ = *N*-acetylneuraminic acid (Neu5Ac), and ■ = *N*-acetyl-glucosamine (GlcNAc)). Mean RT was determined across the four analytical batches (i.e., four measurement days) considering standards and QC samples.

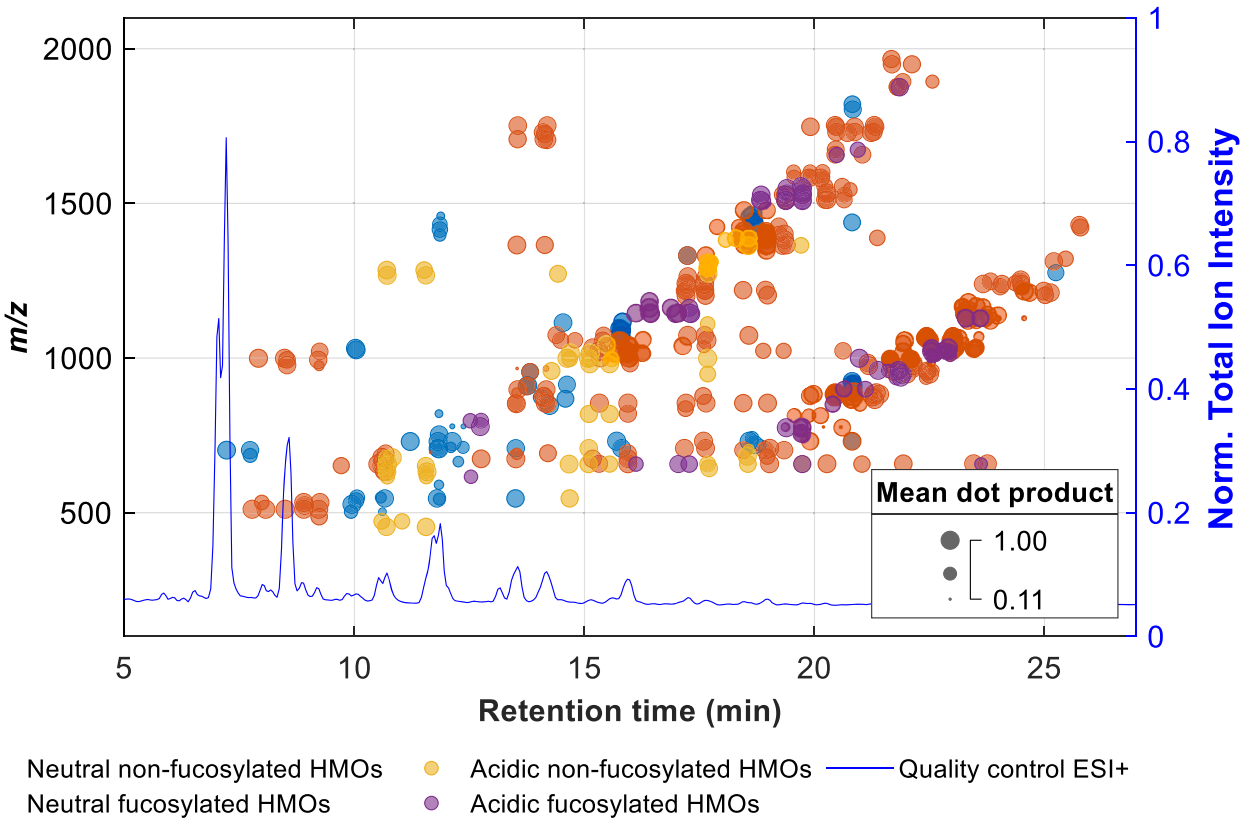


**Fig. 2.** Distribution of annotated HMOs along the *m/z*-retention time space and normalized total ion intensity of a quality control sample in ESI+.

chromatographic system, such as double peaks caused by the presence of anomers and the removal of high-abundance salts and lactose, respectively. On the other hand, fluorescent labeling is employed when combining a fluorescent detector with an MS detector, while permethylation (i.e., replacement of all hydrogens attached to oxygen and nitrogen atoms with methyl groups) is less commonly used. Interestingly, the use of ISs in the quantitation of HMOs is not an extended practice. Thus, the lack of a standardized approach for HMO isolation hinders the comparison of HMO levels across studies. The present work adheres to common practices, including fat and protein removal as well as porous graphited carbon-SPE purification of the HMO fraction. Additionally, it employs an IS, which aids in the accurate quantitation of HMOs. However, the use of a PGC-SPE led to the loss of 3-FL, what other studies overcome by measuring 3-FL separately (Gu et al., 2021). Chromatographic separation is achieved using HILIC, which, along with the use of a porous graphitic carbon column, represents one of the commonly employed approaches for HMO separation. Notably, the total runtime of this method (32 min) is shorter than the average runtime of comparable methods (50 min).

One of the strengths of the present method is the use of polarity switching, which enables both positive and negative ionization of HMOs in a single run, thereby saving time and reducing costs. Additionally, the hybrid approach facilitates both the quantitation of specific (targeted) and the putative identification of additional (untargeted) HMOs, resulting in a total of 110 annotated HMOs. This places the present work among the most comprehensive in terms of the number of HMOs identified per total runtime of analysis. Furthermore, the use of a publicly available library, as opposed to an in-house library, allows for broader reproducibility and accessibility, enhancing its applicability across different research settings.

However, the methodology was developed using only eight standards and relies on the use of a unique spectral database, which may limit the accuracy of HMO identification compared to methodologies that incorporate a more extensive range of standards, potentially affecting the reliability of quantitative and qualitative assessments. Regarding HMO profiling across different populations, this study was conducted in Spain with a limited number of participants, what may lack of representativity compared with other studies involving greater number of samples and participants. However, it contributes to the evaluation of HMOs in the European population as approximately 40 % of the studies considered for comparison were conducted with Asian populations.

While it should be noted that the present comparison is limited to works published between January 1, 2018, and November 1, 2024, and constrained by the query "Human Milk Oligosaccharides liquid chromatography mass spectrometry" within a single database, which may exclude or overlook other methodologies or advancements relevant to HMO analysis, the present methodology represents a strong compromise between depth of analysis and practical efficiency and adds valuable information on HMO profiles found in the Mediterranean area.

### 3.2. *Quantitative analysis of HMOs in DHM samples*

DHM samples ($N$ = 40) were provided by 11 healthy volunteers recruited at the HM bank. For all quantified HMOs as well as for total HMOs (i.e., the sum of concentrations of the set of HMOs quantified), a decreasing trend along lactation was observed, with exception of 3′-SL and LNDFH I (see Fig. 4). Both observations are in accordance with previous results (Csernák et al., 2020; Nijman et al., 2018; Plows et al., 2021; Sprenger et al., 2017), even though Plows et al. (2021) reported no change with time for 2′-FL and DSLNT. It should be noted that in this work, estimation of lactation stage of DHM samples is subjected to a certain inaccuracy due to operational procedures embedded in HM banks, intrinsic interindividual variability, and non-homogeneous distribution of lactation stages and number of DHM batches among donors. Hence, longitudinal changes observed here need to be handled with caution.

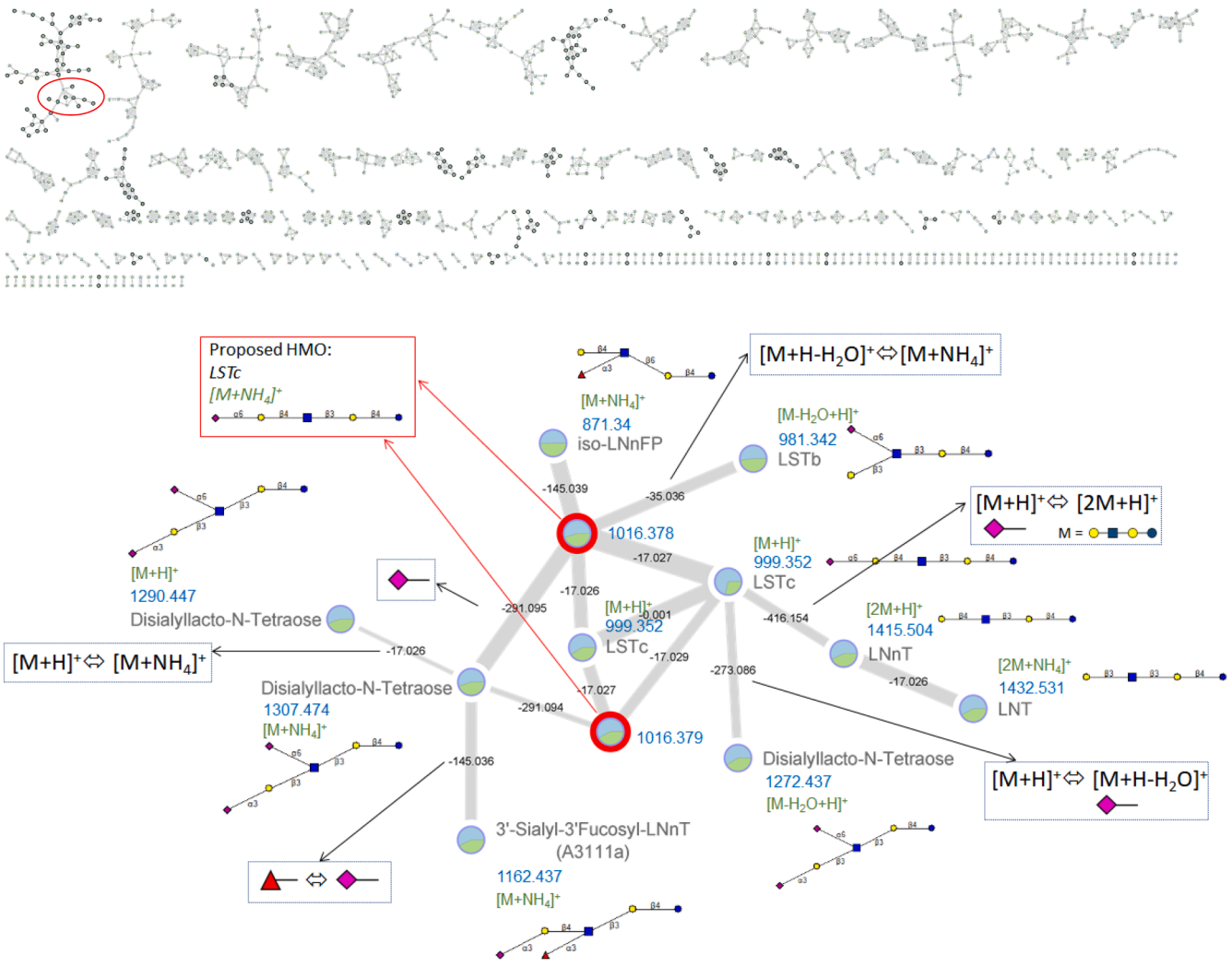


**Fig. 3.** (Top) FBMN of HMOs in the positive mode. The nodes containing annotated HMOs are circled in thick black. (Bottom) Network extracted from FBMN. Note: Each node represents one fragmentation spectrum from a detected compound, and the pie charts indicate the relative abundance of each HMO in the pre-pasteurized (blue) and post-pasteurized (green) DHM samples. Edge thickness indicates the relative similarity of MS/MS data between nodes. Nodes circled in red are not annotated, but a proposed HMOs is suggested. For symbol nomenclature and HMO abbreviations see Table 1 and Table S3, respectively.

### 3.3. Genetic influence on HMO profiles

Results obtained by the proposed analytical method facilitated the study of factors contributing to inter-individual variability in HMOs, with particular emphasis on genetic variations affecting the activity of FUT2 and FUT3 enzymes. As previously described (Yan et al., 2019), 2′-FL, LDFT, and LNFP I were used as HMOs markers for secretor status and LNFP II, LNDFH I, and LNDFH II to distinguish between Lewis phenotypes. As shown in Fig. 5A–C, three out of eleven donors (i.e. 27 %) presented very low levels or absence of 2′-FL, LDFT, and LNFP I and were identified as non-secretor mothers ($Se^-$): This observed ratio was in accordance with percentages reported in literature (J. Li et al., 2022; Samuel et al., 2019). Considering that FUT3 gene produces Lewis A antigen in $Se^-$ and Lewis B antigen in secretors ($Se^+$), these three $Se^-$ mothers can only be assigned to Le($a^+b^-$) or Le($a^-b^-$) phenotypes. LNFP II, that contains $Le^a$ epitope, allowed us to potentially assign Donor 1 as Le($a^-b^-$) (see Fig. 5D). However, it did not allow to discriminate between Le($a^-b^-$) and Le($a^-b^+$) in secretors as no clear differences between donors were observed. On the other hand, LNDFH II ($Le^a$ epitope) has been described as an ideal marker for distinguishing Le($a^+b^-$) and Le ($a^-b^+$) from Le($a^-b^-$), and jointly with LNDFH I ($Le^b$ epitope) it has been reported to be absent in Le($a^-b^-$) individuals (Totten et al., 2012). According to this, three donors were established as Le($a^-b^-$), two of them being $Se^+$ and one $Se^-$ (Fig. 5E). Thus, the phenotypes expressed in HMOs of donors participating in this study were distributed as follows: one Le($a^-b^-$), $Se^-$ (i.e., 9 %); two Le($a^+b^-$), $Se^-$ (i.e., 18 %); six Le ($a^-b^+$), $Se^+$ (i.e., 55 %); and two Le($a^-b^-$), $Se^+$ (i.e., 18 %). This distribution aligns with previous findings involving European population (Mank et al., 2020). Notwithstanding, it should be mentioned that the FUT activity in the synthesis of milk sugars might differ from what is expected based on serological Le blood group determination (Blank et al., 2012).

Furthermore, HMO diversity was estimated through the Simpson's Index of Diversity (see Eq. (1)) and its correlation with postnatal age was assessed (see Fig. 6). For DHM samples, the Simpson's Index of Diversity ranged between 0.27 and 0.77 with a median value of 0.66. HMO diversity diminished with time (Fig. 6, left) and this trend was more noticeable when only secretor mothers were considered (Fig. 6, right). Hence, DHM samples from secretors presented a unique HMO diversity that is also time dependent, and suggests different biological functions and mechanisms by which they may exert an influence on the infant's microbiome and immune maturation and on their susceptibility to infections (Ayechu-Muruzabal et al., 2018). This may have practical implications for HM banks, since the secretor status of mothers is generally not assessed.

**Table 2**
Sample preparation and analysis of HMOs in HM samples described in original articles published between January 1, 2018, to November 1, 2024.

| | Sample preparation | | | | | | | | | | Sample analysis | | | | | | | Cohort | | |
|---|---|---|---|---|---|---|---|---|---|---|---|---|---|---|---|---|---|---|---|---|
| Reference | IS addition | Homogenization (Ultrasounds) | Water dilution | Defatting through cold centrifugation | Deproteinization through organic solvent precipitation | Reduction | SPE purification | Ultrafiltration | Filtration | Fluorescent labeling | Permethylation | Chromatrophic separation | Runtime (min) | Detection | Approach | No. of HMOs standards | No. of annotated / identified HMOs | Spectral database | No. Samples | No. Participants | Geographical region |
| **Present work** | | | | | | | | | | | | **HILIC** | **32** | **ESI(+/-)-MS/MS** | **untargeted & targeted** | **8** | **110** | **NIST milk oligosaccharide library** | **80** | **11** | **Spain** |
| (Remoroza et al., 2018) | | | | | | | | | | | | HILIC | 65 | ESI(+/-)-MS/MS | database generation | 50 | 74 | NIST milk oligosaccharide library | 1 | 0 | SRM 1953 |
| (McJarrow et al., 2019) | | | | | | | | | | | | HILIC | 19 | ESI(-)-MRM-MS/MS | targeted | 1 | 12 | | 81 | unk. | MISC cohort (United Arab Emirates) |
| (Zhang et al., 2019) | | | | | | | | | | | | HILIC | 35 | ESI(+)-MRM-MS/MS | targeted | 12 | 12 | | 61 | 61 | China |
| (Biddulph et al., 2023) | | | | | | | | | | | | HILIC | 35 | ESI(+)-MRM-MS/MS | targeted | 20 | 13 | | 101 | 101 | Australia |
| (Shang et al., 2022) | | | | | | | | | | | | HILIC | 35 | ESI(+)-MRM-MS/MS | targeted | 21 | 19 | | 31 | 49 | China |
| (Siziba et al., 2021) | | | | | | | | | | | | HILIC | 25 | ESI(-)-MRM-MS/MS | targeted | 8 | 16 | | 1203 | 970 | Ulm SPATZ Health Study (Germany) |
| (J. Li et al., 2022) | | | | | | | | | | | | HILIC | 15 | ESI(-)-MRM-MS/MS | targeted | 23 | 23 | | 251 | 251 | China |
| (R. Li et al., 2023) | | | | | | | | | | | | HILIC | 55 | ESI(+)-MS/MS & ESI (-)-MS/MS | untargeted | unk. | 70 | in-house library | 5 | unk. | China |
| (Hou et al., 2024) | | | | | | | | | | | | HILIC | 8 | ESI(-)-MRM-MS/MS | targeted | 5 | 5 | | 196 | 196 | China |

| | Sample preparation | | | | | | | | | | Sample analysis | | | | | | | Cohort | | |
|---|---|---|---|---|---|---|---|---|---|---|---|---|---|---|---|---|---|---|---|---|
| Reference | IS addition | Homogenization (Ultrasounds) | Water dilution | Defatting through cold centrifugation | Deproteinization through organic solvent precipitation | Reduction | SPE purification | Ultrafiltration | Filtration | Fluorescent labeling | Permethylation | Chromatrophic separation | Runtime (min) | Detection | Approach | No. of HMOs standards | No. of annotated / identified HMOs | Spectral database | No. Samples | No. Participants | Geographical region |
| (Austin & Bénet, 2018) | | | | | | | | | | | | HILIC | 110 | ESI(-)-MS | targeted | 10 | 23 | | 3 | 10 | a pooled HM samples from Lee Biosolutions |
| (X. Wang et al., 2022) | | | | | | | | | | | | HILIC | 55 | ESI(+)-MRM-MS/MS | targeted | 13 | 13 | | 99 | 99 | China |
| (Lang et al., 2021) | | | | | | | | | | | | HILIC & PGC | 150 | ESI(+)-MS & ESI (-)-MS/MS | untargeted | unk. | unk. | GlycoWorkBench | 1 | 13 | China |
| (Nijman et al., 2018) | | | | | | | | | | | | nanoLC -Chip (PGC) | 45 | ESI(+)-MS/MS | untargeted | 9 | 130 | in-house library | 20 | 10 | USA |
| (Fan et al., 2023) | | | | | | | | | | | | nanoLC -Chip (PGC) | 80 | ESI(+)-MS/MS | untargeted | unk. | 25 | in-house library | 392 | 392 | STRONG Kids 2 cohort (USA) |
| (Astono et al., 2024) | | | | | | | | | | | | nanoLC -Chip (PGC) | 80 | ESI(+)-MS/MS | untargeted | 1 | 51 | in-house library | 90 | 90 | MaInHealth cohort (Denkmark) |
| (Borewicz et al., 2019) | | | | | | | | | | | | PGC¥ | 65 | ESI-MS (mode not specified) | targeted | unk. | 17 | | 121 | 121 | KOALA birth cohort (the Netherlands) |
| (Barnett et al., 2023) | | | | | | | | | | | | PGC | 66 | ESI-MS (mode not specified) | targeted | 15 | 15 | | 247 | 247 | KOALA birth cohort (the Netherlands) |
| (Gu et al., 2021) | | | | | | | | | | | | PGC¥ | 35 | ESI(-)-MS | targeted | 17 | 17 | | 20 | 20 | KOALA birth cohort (the Netherlands) |
| (Willemsen et al., 2023) | | | | | | | | | | | | PGC¥ | 35 | ESI(-)-MS | targeted | unk. | 24 | | 63 | 63 | BINGO study (the Netherlands) |
| (Tonon, De Morais, et al., 2019) | | | | | | | | | | | | PGC | 55 | ESI(-)-SIM-MS | targeted | 16 | 16 | | 78 | unk. | Brazil |
| (Tonon, Miranda, et al., 2019) | | | | | | | | | | | | PGC | 55 | ESI(-)-SIM-MS | targeted | 16 | 16 | | 41 | 41 | Brazil |
| (Mank et al., 2019) | | | | | | | | | | | | PGC | 18 | ESI(-)-MRM-MS/MS | targeted | 23 | 10 | | 4 | 4 | Germany |
| (Mank et al., 2020) | | | | | | | | | | | | PGC | 18 | ESI(-)-MRM-MS/MS | targeted | 23 | 20 | | 60 | 30 | Germany |
| (Csernák et al., 2020) | | | | | | | | | | | | PGC | 17 | ESI(-)-MRM-MS/MS | targeted | 2 | 2 | | 20 | 1 | unk. (Hungary) |

| | Sample preparation | | | | | | | | | | Sample analysis | | | | | | | Cohort | | |
|---|---|---|---|---|---|---|---|---|---|---|---|---|---|---|---|---|---|---|---|---|
| Reference | IS addition | Homogenization (Ultrasounds) | Water dilution | Defatting through cold centrifugation | Deproteinization through organic solvent precipitation | Reduction | SPE purification | Ultrafiltration | Filtration | Fluorescent labeling | Permethylation | Chromatrophic separation | Runtime (min) | Detection | Approach | No. of HMOs standards | No. of annotated / identified HMOs | Spectral database | No. Samples | No. Participants | Geographical region |
| (Zhu et al., 2024) | | | | | | | | | | | | PGC | 45 | ESI(-)-MRM-MS/MS | targeted | 20 | 20 | | 228 | 96 | China |
| (M. Wang et al., 2020) | | | | | | | | | | | | PGC | 45 | ESI(+)-MS | targeted | 1 | 23 | | 464 | 116 | Maternal and Infants Nutrition Cohort (China) |
| (Y. Chen et al., 2023) | | | | | | | | | | | | PGC | 60 | ESI(+)-MS/MS | targeted | 4 | 4 | | 86 | 103 | SMART Gen HK (China) |
| (Yan et al., 2019) | | | | | | | | | | | | ERLIC | 34 | ESI(-)-MS/MS | targeted | 12 | 27 | | 14 | 12 | China |
| (Liu et al., 2021) | | | | | | | | | | | | ERLIC | 55 | ESI(-)-MS/MS | targeted | 12 | 27 | | 28 | 39 | China |
| (Cho et al., 2020) | | | | | | | | | | | | nanoLC (C18) | 90 | ESI(+)-MS/MS | untargeted | unk. | unk. | GlycoWorkBench | 1 | 1 | unk. (China) |
| (Porfirio et al., 2020) | | | | | | | | | | | | nanoLC (C18) | 40 | NSI(+)-MS/MS | untargeted | 6 | 102 | GlycoWorkBench | 130 | 130 | Bangladesh |

NOTE: CID, collision induced; ERLIC, mixed-mode electrostatic repulsion/hydrophilic interaction liquid chromatography; ESI, electrospray ionization; HILIC, hydrophilic interaction liquid chromatography; IS, internal standard; MRM, multiple reaction monitoring; MS, mass spectrometry; NSI, nanospray ionization; PGC, porous graphited carbon; SIM, single ion monitoring; SRM, standard reference material; unk., unknown. The different steps followed during the sample preparation are presented in the frequently encountered order, but it may vary depending on the particular approach.
¥Quantitation of the PGC-SPE fraction containing 3-FL is accomplished by high-performance anion-exchange chromatography-pulsed amperometric detection (HPAEC-PAD) (Astono et al., 2024; Austin & Bénet, 2018; Barnett et al., 2023; Biddulph et al., 2023; Borewicz et al., 2019; Chen et al., 2023; Cho et al., 2020; Hou et al., 2024; Lang et al., 2021; Li et al., 2023; Liu et al., 2021; Mank et al., 2019; McJarrow et al., 2019; Shang et al., 2022; Tonon et al., 2019a; Wang et al., 2022; Willemsen et al., 2023; Zhang et al., 2019; Zhu et al., 2024).

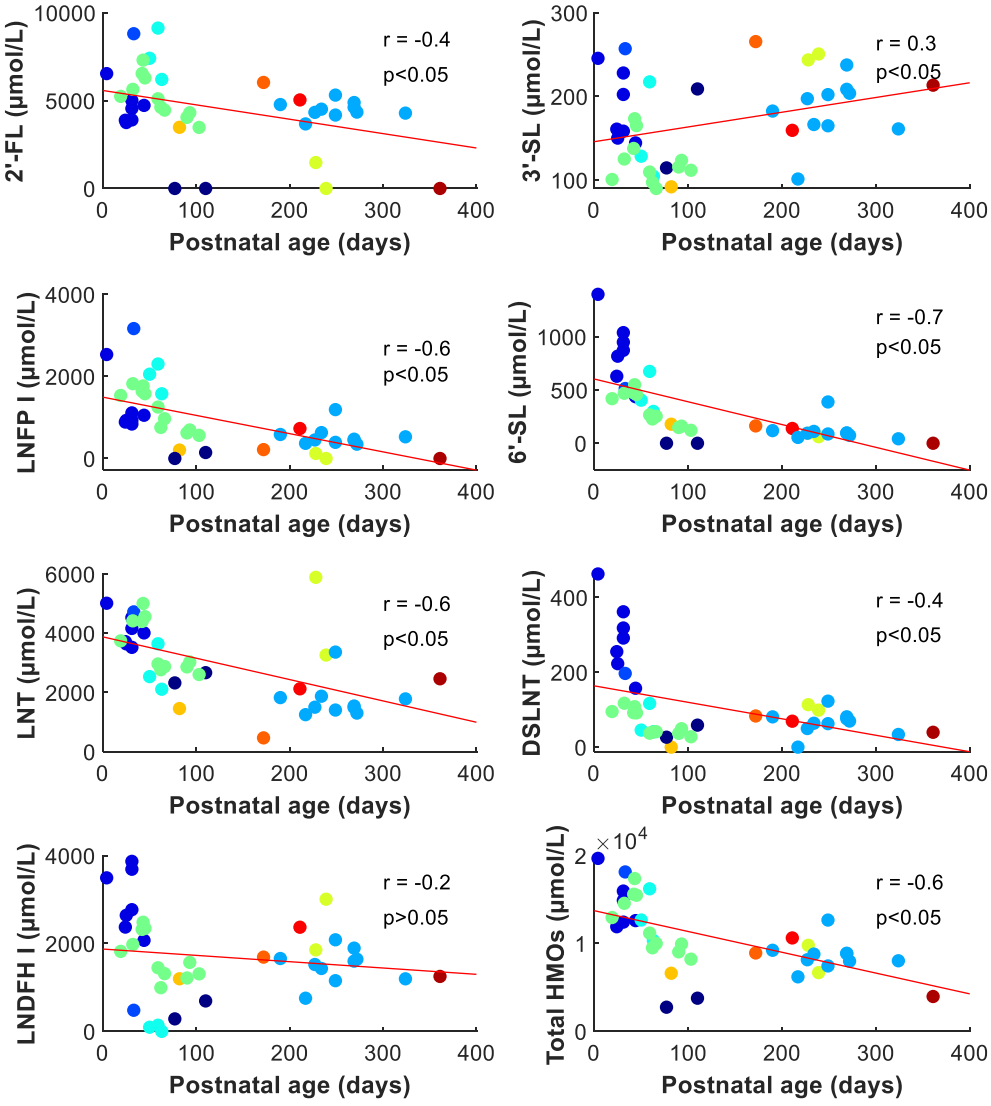


**Fig. 4.** Change of quantified HMOs in DHM samples prior to pasteurization correlated with time after delivery. Samples have been coloured according to milk donor. See Table 1 for abbreviations.

### 3.4. Impact of holder pasteurization on HMOs

The effect of pasteurization on detected HMOs was assessed. The thermal process had no effect on quantified HMOs (data not shown, *p*-values >0.05, Wilcoxon signed-rank test), in accordance with findings reported in literature (Bertino et al., 2008; Hahn et al., 2019). **Figure S5** shows volcano plot of *p*-values (Wilcoxon signed-rank test) vs log2 fold-change (FC) of median values of annotated HMOs in DHM samples before (Pre) and after (Post) pasteurization, where no significant differences between the groups could be observed. To our knowledge, this is the first study in which the pasteurization effect is broadly analysed considering over 100 HMOs, since previous studies only focused on a small number of HMOs (up to 33) (Hahn et al., 2019). On the other hand, Fig. 3 (bottom) shows connected nodes extracted from the FBMN (red circle), where pie charts indicate the relative abundance of each HMO in the pre-pasteurized (blue) and post-pasteurized (green) DHM samples. As it can be observed, the abundance of HMOs was comparable in agreement with the results derived from the univariate analysis of quantified and annotated HMOs (see **Figure S5**).

## 4. Conclusions

The developed hybrid UPLC-MS method enables the quantitative analysis of a subset of HMOs and, simultaneously, the annotation and relative quantification of HMOs in a single run. Furthermore, this is the first study to apply FBMN to elucidate novel HMO structures using the

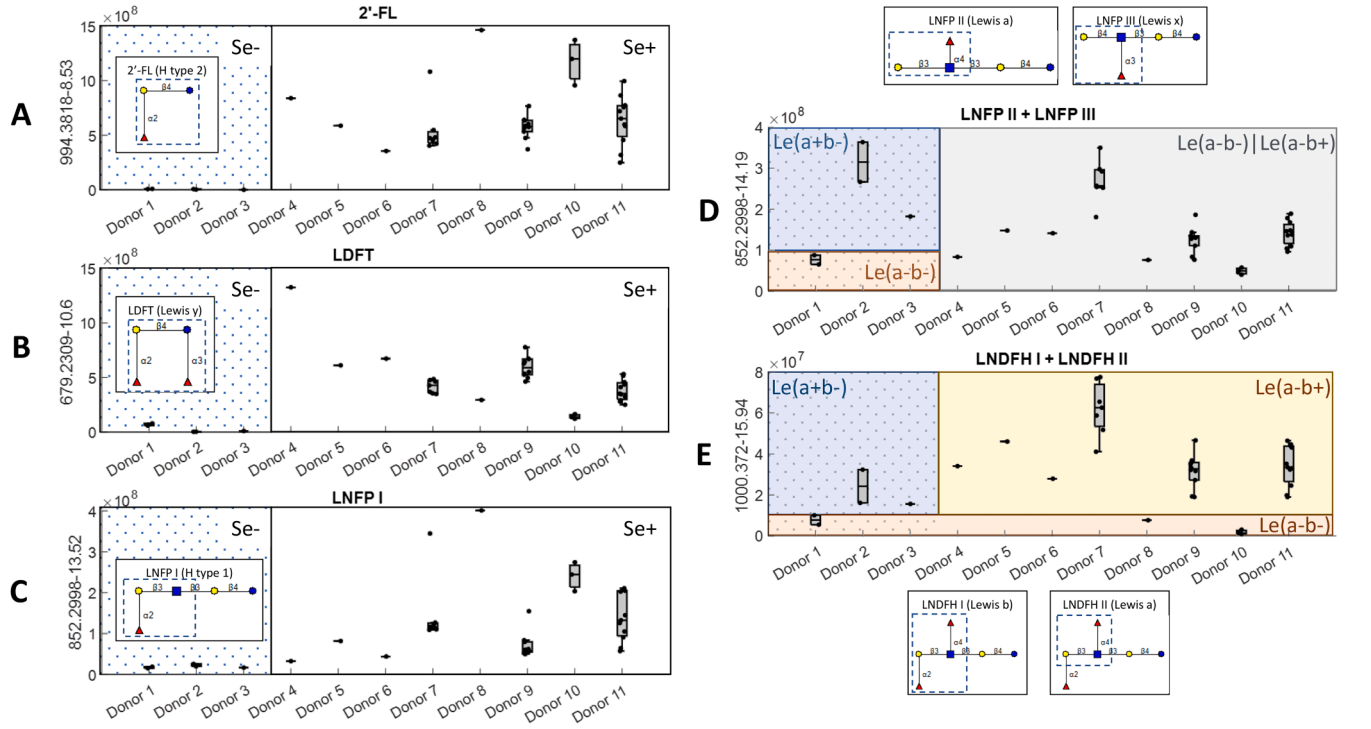


**Fig. 5.** Intensity of LC-MS features corresponding to 2′-FL (A), LDFT (B), LNFP I (C), LNFP II + LNFP III (D), and LNDFH *I* + LNDFH II (D) in DHM samples grouped by donor. Inference of secretor status (i.e., secretor ($Se^+$) and non-secretor ($Se^-$)) has been delimited with plain and dotted background, respectively; and inference of Lewis phenotypes with colors: Le($a^+b^-$) in blue, Le($a^-b^+$) in yellow and Le($a^-b^-$) in red. H type 1, $Le^a$, $Le^b$, $Le^x$, and $Le^y$ epitopes on HMOs have been boxed with a dashed line. Note that $Le^y$ in LDFT is a glucose analog of these Lewis antigens.

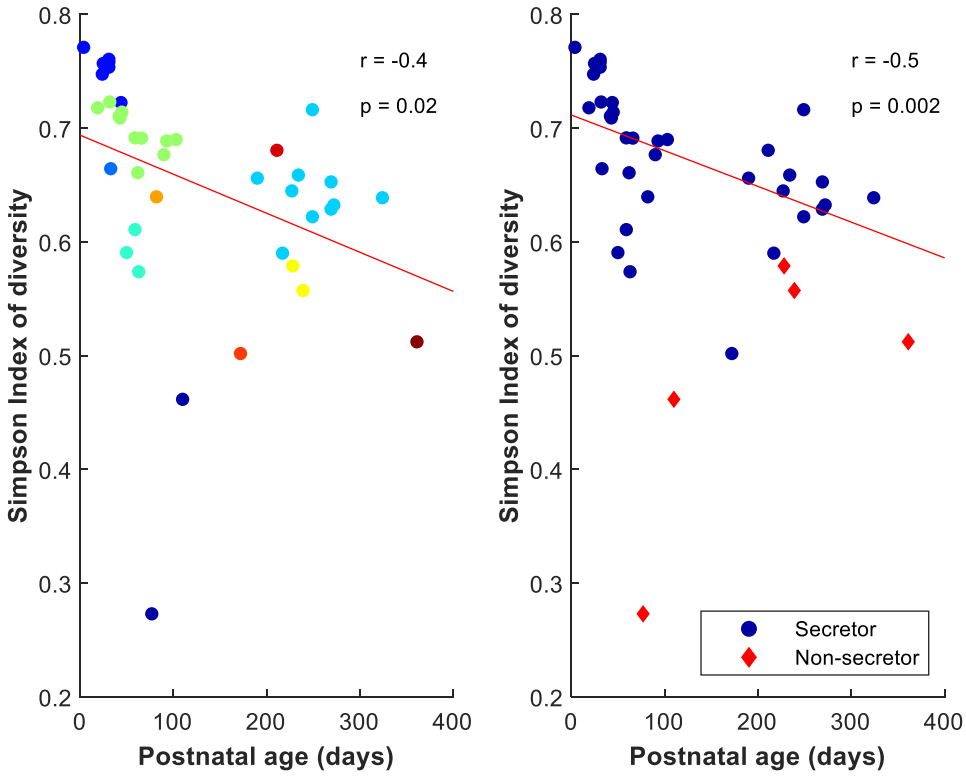


**Fig. 6.** Correlation of the Simpson's Index of Diversity and time after delivery of both secretor and non-secretor donors (each colour represents samples from one donor) (left) and of secretor donors (right).

NIST Milk Oligosaccharide MS Library, broadening the scope of HMO profiling in clinical research. The suitability and robustness of the approach for clinical research allowing the analysis and comparison of larger numbers of samples (i.e., 80 HM samples) was demonstrated. The application of the developed method to the analysis of HM allowed the effective assignment of secretor and Lewis status of donors and provided evidence that (i) concentrations of several HMOs as well as HMO diversity may decrease with increasing postnatal age of the infant and (ii) thermal treatment does not significantly affect the levels of a broad panel of HMOs in HM. The developed methodology will be applied in future efforts to study differences in milk composition between mothers from term and preterm infants, as well as for a longitudinal survey of HMO concentrations across different lactation stages. Findings might be of practical importance for protocols implemented at HM banks for donor-patient matching or for HM supplementation. While it has been demonstrated that the development of powerful methodologies enabling thorough analysis of HMO profiles is possible, such methodologies are not effective for decision-making in clinical practice, as they require sophisticated instrumentation and appropriate facilities, as well as qualified laboratory personnel. Therefore, a need for the development of alternative methodologies that allow for a quick, on-site assessment of HMO profiles by clinical staff (Chung et al., 2022) is identified to facilitate the clinical translation and application in real-life settings.

## Funding

This work was supported by the *Instituto de Salud Carlos III* (ISC III), Spain, and co-funded by the European Union [grant numbers PI23/00202 and CPII21/00003], *Generalitat Valenciana* [project number GV/2021/186], grant CNS2022-135398 funded by MCIN/AEI/10.13039/501100011033 and, as appropriate, by "European Union NextGenerationEU/PRTR", and the European Union's Horizon 2020 Research and Innovation Programme through the Nutrishield project (https://nutrishield-project.eu/) [Grant Agreement No 818110]. V.N.E. acknowledges the financial support by the grant PRE2021-098833 from the Spanish MCIN/AEI/10.13039/501100011033 and the FSE+.

## CRediT authorship contribution statement

**Víctor Navarro-Esteve:** Writing – review & editing, Writing – original draft, Validation, Software, Methodology, Investigation, Formal analysis, Data curation. **Anna Zöchner:** Writing – review & editing, Writing – original draft, Validation, Methodology, Investigation, Formal analysis, Data curation. **Marta Roca:** Writing – review & editing, Writing – original draft, Methodology, Formal analysis, Data curation. **Anna Parra-Llorca:** Writing – review & editing, Writing – original draft, Methodology, Investigation. **Alba Moreno-Giménez:** Writing – review & editing, Writing – original draft, Methodology, Investigation. **Laura Campos-Berga:** Writing – review & editing, Writing – original draft, Methodology, Investigation. **María Jesús Vaya:** Writing – review & editing, Writing – original draft, Methodology, Investigation. **Máximo Vento:** Writing – review & editing, Writing – original draft, Visualization, Supervision, Methodology, Investigation, Funding acquisition, Conceptualization. **Pilar Sáenz González:** Writing – review & editing, Writing – original draft, Visualization, Supervision, Methodology, Investigation, Funding acquisition, Conceptualization. **María Gormaz:** Writing – review & editing, Writing – original draft, Visualization, Supervision, Methodology, Investigation, Funding acquisition, Conceptualization. **Isabel Ten-Doménech:** Writing – review & editing, Writing – original draft, Visualization, Validation, Supervision, Software, Methodology, Investigation, Funding acquisition, Formal analysis, Data curation, Conceptualization. **Julia Kuligowski:** Writing – review & editing, Writing – original draft, Visualization, Validation, Supervision, Software, Methodology, Investigation, Formal analysis, Data curation, Conceptualization. **Guillermo Quintás:** Writing – review & editing, Writing – original draft, Visualization, Validation, Supervision, Software, Methodology, Investigation, Formal analysis, Data curation, Conceptualization.

## Declaration of competing interest

The authors declare that they have no known competing financial interests or personal relationships that could have appeared to influence the work reported in this paper.

## Acknowledgements

The authors are grateful to mothers who agreed to participate in this study. The authors would like to thank Amparo Ramón and Antonia Gázquez from the human milk bank of Hospital La Fe for their help and availability and Dr. Ming Wang for his help with the GNPS platform.

## Supplementary materials

Supplementary material associated with this article can be found, in the online version, at doi:10.1016/j.carpta.2024.100644.

## Data availability

The MS data has been deposited on MassIVE public repository with code: MSV000090546.

## References

Abikhodr, A. H., Warnke, S., Ben Faleh, A., & Rizzo, T. R. (2024). Combining liquid chromatography and cryogenic IR spectroscopy in real time for the analysis of oligosaccharides. *Analytical Chemistry, 96*(4), 1462–1467. https://doi.org/10.1021/acs.analchem.3c03578

Astono, J., Huang, Y.-P., Sundekilde, U. K., & Barile, D. (2024). Human milk oligosaccharide profiles remain unaffected by maternal pre-pregnancy body mass index in an observational study. *Frontiers in Nutrition, 11*, Article 1455251. https://doi.org/10.3389/fnut.2024.1455251

Auer, F., Jarvas, G., & Guttman, A. (2021). Recent advances in the analysis of human milk oligosaccharides by liquid phase separation methods. *Journal of Chromatography B, 1162*, Article 122497. https://doi.org/10.1016/j.jchromb.2020.122497

Austin, S., & Bénet, T. (2018). Quantitative determination of non-lactose milk oligosaccharides. *Analytica Chimica Acta, 1010*, 86–96. https://doi.org/10.1016/j.aca.2017.12.036

Autran, C. A., Kellman, B. P., Kim, J. H., Asztalos, E., Blood, A. B., Spence, E. C. H., Patel, A. L., Hou, J., Lewis, N. E., & Bode, L. (2018). Human milk oligosaccharide composition predicts risk of necrotising enterocolitis in preterm infants. *Gut, 67*(6), 1064–1070. https://doi.org/10.1136/gutjnl-2016-312819

Ayechu-Muruzabal, V., van Stigt, A. H., Mank, M., Willemsen, L. E. M., Stahl, B., Garssen, J., & van't Land, B. (2018). Diversity of human milk oligosaccharides and effects on early life immune development. *Frontiers in Pediatrics, 6*, 239. https://doi.org/10.3389/fped.2018.00239

Barnett, D. J. M., Endika, M. F., Klostermann, C. E., Gu, F., Thijs, C., Nauta, A., Schols, H. A., Smidt, H., Arts, I. C. W., & Penders, J. (2023). Human milk oligosaccharides, antimicrobial drugs, and the gut microbiota of term neonates: Observations from the KOALA birth cohort study. *Gut Microbes, 15*(1), Article 2164152. https://doi.org/10.1080/19490976.2022.2164152

Belfort, M. B., & Inder, T. E. (2022). Human Milk and Preterm Infant Brain Development: A Narrative Review. *Clinical Therapeutics, 44*(4), 612–621. https://doi.org/10.1016/j.clinthera.2022.02.011

Bertino, E., Coppa, G. V., Giuliani, F., Coscia, A., Gabrielli, O., Sabatino, G., Sgarrella, M., Testa, T., Zampini, L., & Fabris, C. (2008). Effects of holder pasteurization on human milk oligosaccharides. *International Journal of Immunopathology and Pharmacology, 21*(2), 381–385. https://doi.org/10.1177/039463200802100216

Biddulph, C., Holmes, M., Tran, T. D., Kuballa, A., Davies, P. S. W., Koorts, P., & Maher, J. (2023). Associations between maternal nutrition and the concentrations of human milk oligosaccharides in a cohort of healthy Australian lactating women. *Nutrients, 15*(9), 2093. https://doi.org/10.3390/nu15092093

Blank, D., Dotz, V., Geyer, R., & Kunz, C. (2012). Human milk oligosaccharides and Lewis blood group: Individual high-throughput sample profiling to enhance conclusions from functional studies. *Advances in Nutrition, 3*(3), 440S–449S. https://doi.org/10.3945/an.111.001446

Boquien, C.-Y. (2018). Human milk: An ideal food for nutrition of preterm newborn. *Frontiers in Pediatrics, 6*, 295. https://doi.org/10.3389/fped.2018.00295

Borewicz, K., Gu, F., Saccenti, E., Arts, I. C. W., Penders, J., Thijs, C., Van Leeuwen, S. S., Lindner, C., Nauta, A., Van Leusen, E., Schols, H. A., & Smidt, H. (2019). Correlating infant fecal microbiota composition and human milk oligosaccharide consumption

by microbiota of 1-month-old breastfed infants. *Molecular Nutrition & Food Research, 63*(13), Article 1801214. https://doi.org/10.1002/mnfr.201801214

Broadhurst, D., Goodacre, R., Reinke, S. N., Kuligowski, J., Wilson, I. D., Lewis, M. R., & Dunn, W. B. (2018). Guidelines and considerations for the use of system suitability and quality control samples in mass spectrometry assays applied in untargeted clinical metabolomic studies. *Metabolomics : Official Journal of the Metabolomic Society, 14*(6), 72. https://doi.org/10.1007/s11306-018-1367-3

Catenza, K. F., & Donkor, K. K. (2021). Recent approaches for the quantitative analysis of functional oligosaccharides used in the food industry: A review. *Food Chemistry, 355*, Article 129416. https://doi.org/10.1016/j.foodchem.2021.129416

Chen, Q., Mueed, A., Zhu, L., Deng, Z., Peng, H., Li, H., & Zhang, B. (2024). HPLC-QQQ-MS/MS-based authentication and determination of free and bound sialic acids content inhuman, bovine, sheep, goat milk, and infant formula. *Journal of Food Science, 89*, 4178–4198. https://doi.org/10.1111/1750-3841.17161

Chen, Y., Jiachi Chiou, A., Sze Tin Leung, A., Ching Ching Chan, K., Kam Chang, M., Sze Cheng, N., Kay Sheung Chan, P., Sau Wong, M., Hung Tam, W., & Fan Leung, T. (2023). Human milk oligosaccharides in Chinese lactating mothers and relationship with allergy development in offspring. *Asian Pacific Journal of Allergy and Immunology*. https://doi.org/10.12932/AP-110922-1453

Cho, B. G., Peng, W., & Mechref, Y. (2020). Separation of permethylated O-glycans, free oligosaccharides, and glycosphingolipid-glycans using porous graphitized carbon (PGC) column. *Metabolites, 10*(11), 433. https://doi.org/10.3390/metabo10110433

Chung, S., Bode, L., & Hall, D. A. (2022). Point-of-care human milk testing for maternal secretor status. *Analytical and Bioanalytical Chemistry, 414*(10), 3187–3196. https://doi.org/10.1007/s00216-021-03697-7

Csernák, O., Rácz, B., Alberti, Á., & Béni, S. (2020). Quantitative analysis of 3'- and 6'-sialyllactose in human milk samples by HPLC-MS/MS: A validated method for the comparison of two consecutive lactation periods in the same woman. *Journal of Pharmaceutical and Biomedical Analysis, 184*, Article 113184. https://doi.org/10.1016/j.jpba.2020.113184

Duchon, J., Barbian, M. E., & Denning, P. W. (2021). Necrotizing enterocolitis. *Clinics in Perinatology, 48*(2), 229–250. https://doi.org/10.1016/j.clp.2021.03.002

Fan, Y., Vinjamuri, A., Tu, D., Lebrilla, C. B., & Donovan, S. M. (2023). Determinants of human milk oligosaccharides profiles of participants in the STRONG kids 2 cohort. *Frontiers in Nutrition, 10*, Article 1105668. https://doi.org/10.3389/fnut.2023.1105668

Gu, F., Kate, G. A. T., Arts, I. C. W., Penders, J., Thijs, C., Lindner, C., Nauta, A., Van Leusen, E., Van Leeuwen, S. S., & Schols, H. A. (2021). Combining HPAEC-PAD, PGC-LC–MS, and 1D $^{1}$H NMR to investigate metabolic fates of human milk oligosaccharides in 1-month-old infants: A pilot study. *Journal of Agricultural and Food Chemistry, 69*(23), 6495–6509. https://doi.org/10.1021/acs.jafc.0c07446

Hahn, W., Kim, J., Song, S., Park, S., & Kang, N. M. (2019). The human milk oligosaccharides are not affected by pasteurization and freeze-drying. *The Journal of Maternal-Fetal & Neonatal Medicine, 32*(6), 985–991. https://doi.org/10.1080/14767058.2017.1397122

Hou, H., Wang, M., Yang, S., Yang, X., Sun, W., Sun, X., Guo, Q., Debrah, A. A., & Zhenxia, D. (2024). Evaluation of prebiotic glycan composition in human milk and infant formula: Profile of Galacto-oligosaccharides and absolute quantification of major milk oligosaccharides by UPLC-cyclic IM-MS and UPLC-MS/MS. *Journal of Agricultural and Food Chemistry, 72*(14), 7980–7990. https://doi.org/10.1021/acs.jafc.4c00810

Hutchins, P. D., Russell, J. D., & Coon, J. J. (2018). LipiDex: An integrated software package for high-confidence lipid identification. *Cell Systems, 6*(5). https://doi.org/10.1016/j.cels.2018.03.011, 621-625.e5.

Kessner, D., Chambers, M., Burke, R., Agus, D., & Mallick, P. (2008). ProteoWizard: Open source software for rapid proteomics tools development. *Bioinformatics (Oxford, England), 24*(21), 2534–2536. https://doi.org/10.1093/bioinformatics/btn323

Kuligowski, J., Sánchez-Illana, Á., Sanjuán-Herráez, D., Vento, M., & Quintás, G. (2015). Intra-batch effect correction in liquid chromatography-mass spectrometry using quality control samples and support vector regression (QC-SVRC). *The Analyst, 140*(22), 7810–7817. https://doi.org/10.1039/c5an01638j

Lang, Y., Zhang, Y., Wang, C., Huang, L., Liu, X., Song, N., Li, G., & Yu, G. (2021). Comparison of different labeling techniques for the LC-MS Profiling of human milk oligosaccharides. *Frontiers in Chemistry, 9*, Article 691299. https://doi.org/10.3389/fchem.2021.691299

Larsson, M. W., Lind, M. V., Laursen, R. P., Yonemitsu, C., Larnkjær, A., Mølgaard, C., Michaelsen, K. F., & Bode, L. (2019). Human milk oligosaccharide composition is associated with excessive weight gain during exclusive breastfeeding-an explorative study. *Frontiers in Pediatrics, 7*, 297. https://doi.org/10.3389/fped.2019.00297

Li, J., Bi, Y., Zheng, Y., Cao, C., Yu, L., Yang, Z., Chai, W., Yan, J., Lai, J., & Liang, X. (2022). Development of high-throughput UPLC-MS/MS using multiple reaction monitoring for quantitation of complex human milk oligosaccharides and application to large population survey of secretor status and Lewis blood group. *Food Chemistry, 397*, Article 133750. https://doi.org/10.1016/j.foodchem.2022.133750

Li, R., Zhou, Y., & Xu, Y. (2023). Comparative analysis of oligosaccharides in the milk of human and animals by using LC-QE-HF-MS. *Food Chemistry: X, 18*, Article 100705. https://doi.org/10.1016/j.fochx.2023.100705

Liu, F., Yan, J., Wang, X., Wang, C., Chen, L., Li, Y., Chen, J., & Guo, H. (2021). Maternal Fucosyltransferase 2 status associates with the profiles of human milk oligosaccharides and the fecal microbiota composition of breastfed infants. *Journal of Agricultural and Food Chemistry, 69*(10), 3032–3043. https://doi.org/10.1021/acs.jafc.0c04575

Louis-Jacques, A. F., & Stuebe, A. M. (2020). Enabling breastfeeding to support lifelong health for mother and child. *Obstetrics and Gynecology Clinics of North America, 47*(3), 363–381. https://doi.org/10.1016/j.ogc.2020.04.001

Mank, M., Hauner, H., Heck, A. J. R., & Stahl, B. (2020). Targeted LC-ESI-MS2 characterization of human milk oligosaccharide diversity at 6 to 16 weeks post-partum reveals clear staging effects and distinctive milk groups. *Analytical and Bioanalytical Chemistry, 412*(25), 6887–6907. https://doi.org/10.1007/s00216-020-02819-x

Mank, M., Welsch, P., Heck, A. J. R., & Stahl, B. (2019). Label-free targeted LC-ESI-MS2 analysis of human milk oligosaccharides (HMOS) and related human milk groups with enhanced structural selectivity. *Analytical and Bioanalytical Chemistry, 411*(1), 231–250. https://doi.org/10.1007/s00216-018-1434-7

Marcobal, A., Barboza, M., Froehlich, J. W., Block, D. E., German, J. B., Lebrilla, C. B., & Mills, D. A. (2010). Consumption of human milk oligosaccharides by gut-related microbes. *Journal of Agricultural and Food Chemistry, 58*(9), 5334–5340. https://doi.org/10.1021/jf9044205

Martínez-Sena, T., Luongo, G., Sanjuan-Herráez, D., Castell, J. V., Vento, M., Quintás, G., & Kuligowski, J. (2019). Monitoring of system conditioning after blank injections in untargeted UPLC-MS metabolomic analysis. *Scientific Reports, 9*(1). https://doi.org/10.1038/s41598-019-46371-w. Article 1.

Masi, A. C., Embleton, N. D., Lamb, C. A., Young, G., Granger, C. L., Najera, J., Smith, D. P., Hoffman, K. L., Petrosino, J. F., Bode, L., Berrington, J. E., & Stewart, C. J. (2021). Human milk oligosaccharide DSLNT and gut microbiome in preterm infants predicts necrotising enterocolitis. *Gut, 70*(12), 2273–2282. https://doi.org/10.1136/gutjnl-2020-322771

McJarrow, P., Radwan, H., Ma, L., MacGibbon, A. K. H., Hashim, M., Hasan, H., Obaid, R. S., Naja, F., Mohamed, H. J. J., Al Ghazal, H., & Fong, B. Y. (2019). Human milk oligosaccharide, phospholipid, and ganglioside concentrations in breast milk from United Arab Emirates Mothers: Results from the MISC Cohort. *Nutrients, 11*(10), 2400. https://doi.org/10.3390/nu11102400

Nijman, R. M., Liu, Y., Bunyatratchata, A., Smilowitz, J. T., Stahl, B., & Barile, D. (2018). Characterization and quantification of oligosaccharides in human milk and infant formula. *Journal of Agricultural and Food Chemistry, 66*(26), 6851–6859. https://doi.org/10.1021/acs.jafc.8b01515

Nolan, L. S., Rimer, J. M., & Good, M. (2020). The role of human milk oligosaccharides and probiotics on the neonatal microbiome and risk of necrotizing enterocolitis: A narrative review. *Nutrients, 12*(10), 3052. https://doi.org/10.3390/nu12103052

Noll, A. J., Gourdine, J.-P., Yu, Y., Lasanajak, Y., Smith, D. F., & Cummings, R. D. (2016). Galectins are human milk glycan receptors. *Glycobiology, 26*(6), 655–669. https://doi.org/10.1093/glycob/cww002

Nothias, L.-F., Petras, D., Schmid, R., Dührkop, K., Rainer, J., Sarvepalli, A., Protsyuk, I., Ernst, M., Tsugawa, H., Fleischauer, M., Aicheler, F., Aksenov, A. A., Alka, O., Allard, P.-M., Barsch, A., Cachet, X., Caraballo-Rodriguez, A. M., Da Silva, R. R., Dang, T., … Dorrestein, P. C. (2020). Feature-based molecular networking in the GNPS analysis environment. *Nature Methods, 17*(9), 905–908. https://doi.org/10.1038/s41592-020-0933-6

Okburan, G., & Kızıler, S. (2023). Human milk oligosaccharides as prebiotics. *Pediatrics & Neonatology, 64*(3), 231–238. https://doi.org/10.1016/j.pedneo.2022.09.017

Peterson, T. L., & Nagy, G. (2021). Toward sequencing the human milk glycome: High-resolution cyclic ion mobility separations of core human milk oligosaccharide building blocks. *Analytical Chemistry, 93*(27), 9397–9407. https://doi.org/10.1021/acs.analchem.1c00942

Plaza-Díaz, J., Fontana, L., & Gil, A. (2018). Human milk oligosaccharides and immune system development. *Nutrients, 10*(8), 1038. https://doi.org/10.3390/nu10081038

Plows, J. F., Berger, P. K., Jones, R. B., Alderete, T. L., Yonemitsu, C., Najera, J. A., Khwajazada, S., Bode, L., & Goran, M. I. (2021). Longitudinal changes in human milk oligosaccharides (HMOs) over the course of 24 months of lactation. *The Journal of Nutrition, 151*(4), 876–882. https://doi.org/10.1093/jn/nxaa427

Plows, J. F., Berger, P. K., Jones, R. B., Yonemitsu, C., Ryoo, J. H., Alderete, T. L., Bode, L., & Goran, M. I. (2020). Associations between human milk oligosaccharides (HMOs) and eating behaviour in Hispanic infants at 1 and 6 months of age. *Pediatric Obesity, 15*(12), e12686. https://doi.org/10.1111/ijpo.12686

Porfirio, S., Archer-Hartmann, S., Moreau, G. B., Ramakrishnan, G., Haque, R., Kirkpatrick, B. D., Petri, W. A., & Azadi, P. (2020). New strategies for profiling and characterization of human milk oligosaccharides. *Glycobiology, 30*(10), 774–786. https://doi.org/10.1093/glycob/cwaa028

Remoroza, C. A., Liang, Y., Mak, T. D., Mirokhin, Y., Sheetlin, S. L., Yang, X., San Andres, J. V., Power, M. L., & Stein, S. E. (2020). Increasing the coverage of a mass spectral library of milk oligosaccharides using a hybrid-search-based bootstrapping method and milks from a wide variety of mammals. *Analytical Chemistry, 92*(15), 10316–10326. https://doi.org/10.1021/acs.analchem.0c00342

Remoroza, C. A., Mak, T. D., De Leoz, M. L. A., Mirokhin, Y. A., & Stein, S. E. (2018). Creating a mass spectral reference library for oligosaccharides in human milk. *Analytical Chemistry, 90*(15), 8977–8988. https://doi.org/10.1021/acs.analchem.8b01176

Samuel, T. M., Binia, A., de Castro, C. A., Thakkar, S. K., Billeaud, C., Agosti, M., Al-Jashi, I., Costeira, M. J., Marchini, G., Martínez-Costa, C., Picaud, J.-C., Stiris, T., Stoicescu, S.-M., Vanpeé, M., Domellöf, M., Austin, S., & Sprenger, N. (2019). Impact of maternal characteristics on human milk oligosaccharide composition over the first 4 months of lactation in a cohort of healthy European mothers. *Scientific Reports, 9*(1), 11767–11776. https://doi.org/10.1038/s41598-019-48337-4

Sánchez-Illana, Á., Pérez-Guaita, D., Cuesta-García, D., Sanjuan-Herráez, J. D., Vento, M., Ruiz-Cerdá, J. L., Quintás, G., & Kuligowski, J. (2018a). Model selection for within-batch effect correction in UPLC-MS metabolomics using quality control—Support vector regression. *Analytica Chimica Acta, 1026*, 62–68. https://doi.org/10.1016/j.aca.2018.04.055

Sánchez-Illana, Á., Piñeiro-Ramos, J. D., Sanjuan-Herráez, J. D., Vento, M., Quintás, G., & Kuligowski, J. (2018b). Evaluation of batch effect elimination using quality

control replicates in LC-MS metabolite profiling. *Analytica Chimica Acta, 1019*, 38–48.

Shang, J., Yang, S., & Meng, X. (2022). Correlations between oligosaccharides in breast milk and the composition of the gut microbiome in breastfed infants. *Journal of Dairy Science, 105*(6), 4818–4828. https://doi.org/10.3168/jds.2021-20928

Shannon, P., Markiel, A., Ozier, O., Baliga, N. S., Wang, J. T., Ramage, D., Amin, N., Schwikowski, B., & Ideker, T. (2003). Cytoscape: A software environment for integrated models of biomolecular interaction networks. *Genome Research, 13*, 2498–2504. https://doi.org/10.1101/gr.1239303

Sizíba, L., Mank, M., Stahl, B., Gonsalves, J., Blijenberg, B., Rothenbacher, D., & Genuneit, J. (2021). Human milk oligosaccharide profiles over 12 months of lactation: The Ulm SPATZ health study. *Nutrients, 13*(6), 1973. https://doi.org/10.3390/nu13061973

Soyyılmaz, B., Mikš, M. H., Röhrig, C. H., Matwiejuk, M., Meszaros-Matwiejuk, A., & Vigsnæs, L. K. (2021). The mean of milk: A review of human milk oligosaccharide concentrations throughout lactation. *Nutrients, 13*(8), 2737. https://doi.org/10.3390/nu13082737

Sprenger, N., Lee, L. Y., De Castro, C. A., Steenhout, P., & Thakkar, S. K. (2017). Longitudinal change of selected human milk oligosaccharides and association to infants' growth, an observatory, single center, longitudinal cohort study. *PLOS ONE, 12*(2), Article e0171814. https://doi.org/10.1371/journal.pone.0171814

Sumner, L. W., Amberg, A., Barrett, D., Beale, M. H., Beger, R., Daykin, C. A., Fan, T. W.-M., Fiehn, O., Goodacre, R., Griffin, J. L., Hankemeier, T., Hardy, N., Harnly, J., Higashi, R., Kopka, J., Lane, A. N., Lindon, J. C., Marriott, P., Nicholls, A. W., … Viant, M. R. (2007). Proposed minimum reporting standards for chemical analysis: Chemical Analysis Working Group (CAWG) metabolomics standards initiative (MSI). *Metabolomics : Official Journal of the Metabolomic Society, 3*(3), 211–221. https://doi.org/10.1007/s11306-007-0082-2

Tautenhahn, R., Patti, G. J., Rinehart, D., & Siuzdak, G. (2012). XCMS Online: A web-based platform to process untargeted metabolomic data. *Analytical Chemistry, 84*(11), 5035–5039. https://doi.org/10.1021/ac300698c

Ten-Doménech, I., Martínez-Sena, T., Moreno-Torres, M., Sanjuan-Herráez, J. D., Castell, J. V., Parra-Llorca, A., Vento, M., Quintás, G., & Kuligowski, J. (2020). Comparing Targeted vs. Untargeted MS2 data-dependent acquisition for peak Annotation in LC-MS metabolomics. *Metabolites, 10*(4), E126. https://doi.org/10.3390/metabo10040126

Tonon, K. M., De Morais, M. B., Abrão, A. C. F. V., Miranda, A., & Morais, T. B. (2019a). Maternal and infant factors associated with human milk oligosaccharides concentrations according to secretor and Lewis phenotypes. *Nutrients, 11*(6), 1358. https://doi.org/10.3390/nu11061358

Tonon, K. M., Miranda, A., Abrão, A. C. F. V., de Morais, M. B., & Morais, T. B. (2019b). Validation and application of a method for the simultaneous absolute quantification of 16 neutral and acidic human milk oligosaccharides by graphitized carbon liquid chromatography – electrospray ionization – mass spectrometry. *Food Chemistry, 274*, 691–697. https://doi.org/10.1016/j.foodchem.2018.09.036

Totten, S. M., Zivkovic, A. M., Wu, S., Ngyuen, U., Freeman, S. L., Ruhaak, L. R., Darboe, M. K., German, J. B., Prentice, A. M., & Lebrilla, C. B. (2012). Comprehensive profiles of human milk oligosaccharides yield highly sensitive and specific markers for determining secretor status in lactating mothers. *Journal of Proteome Research, 11*(12), 6124–6133. https://doi.org/10.1021/pr300769g

Underwood, M. A. (2013). Human milk for the premature infant. *Pediatric Clinics of North America, 60*(1), 189–207. https://doi.org/10.1016/j.pcl.2012.09.008

Urashima, T., Hirabayashi, J., Sato, S., & Kobata, A. (2018). Human milk oligosaccharides as essential tools for basic and application studies on galectins. *Trends in Glycoscience and Glycotechnology, 30*(172), SE51–SE65. https://doi.org/10.4052/tigg.1734.1SE

Wang, M., Carver, J. J., Phelan, V. V., Sanchez, L. M., Garg, N., Peng, Y., Nguyen, D. D., Watrous, J., Kapono, C. A., Luzzatto-Knaan, T., Porto, C., Bouslimani, A., Melnik, A. V., Meehan, M. J., Liu, W.-T., Crüsemann, M., Boudreau, P. D., Esquenazi, E., Sandoval-Calderón, M., … Bandeira, N. (2016). Sharing and community curation of mass spectrometry data with global natural products social molecular networking. *Nature Biotechnology, 34*(8), 828–837. https://doi.org/10.1038/nbt.3597

Wang, M., Zhao, Z., Zhao, A., Zhang, J., Wu, W., Ren, Z., Wang, P., & Zhang, Y. (2020). Neutral human milk oligosaccharides are associated with multiple fixed and modifiable maternal and infant characteristics. *Nutrients, 12*(3), 826. https://doi.org/10.3390/nu12030826

Wang, X., Liu, J., Li, C., Xu, Y., Wang, X., Lu, Y., Zhang, T., Cao, H., Huang, L., & Wang, Z. (2022). Pregnancy-related diseases and delivery mode can affect the content of human milk oligosaccharides: A preliminary study. *Journal of Agricultural and Food Chemistry, 70*(16), 5207–5217. https://doi.org/10.1021/acs.jafc.2c00147

Willemsen, Y., Beijers, R., Gu, F., Vasquez, A. A., Schols, H. A., & De Weerth, C. (2023). Fucosylated human milk oligosaccharides during the first 12 postnatal weeks are associated with better executive functions in toddlers. *Nutrients, 15*(6), 1463. https://doi.org/10.3390/nu15061463

Yan, J., Ding, J., Jin, G., Duan, Z., Yang, F., Li, D., Zhou, H., Li, M., Guo, Z., Chai, W., & Liang, X. (2019). Profiling of human milk oligosaccharides for Lewis epitopes and secretor status by electrostatic repulsion hydrophilic interaction chromatography coupled with negative-ion electrospray tandem mass spectrometry. *Analytical Chemistry, 91*(13), 8199–8206. https://doi.org/10.1021/acs.analchem.9b00687

Zhang, W., Wang, T., Chen, X., Pang, X., Zhang, S., Obaroakpo, J. U., Shilong, J., Lu, J., & Lv, J. (2019). Absolute quantification of twelve oligosaccharides in human milk using a targeted mass spectrometry-based approach. *Carbohydrate Polymers, 219*, 328–333. https://doi.org/10.1016/j.carbpol.2019.04.092

Zhu, L., Peng, X., Li, H., Luo, T., Wang, J., Gao, Y., Deng, Z., Li, J., Li, W., Zheng, L., & Zhang, B. (2024). Systematic characterization of the oligosaccharide profile of human milk in rural areas of central China: Quantitative tracking of human milk oligosaccharide composition during 12 months of lactation. *Journal of Agricultural and Food Chemistry*. https://doi.org/10.1021/acs.jafc.4c07225. acs.jafc.4c07225.